Infection and Drug Resistance

Dovepress
Taylor & Francis Group

Open Access Full Text Article

ORIGINAL RESEARCH

Proteomic Analysis of Cerebrospinal Fluid: Toward the Identification of Biomarkers for Early Central Nervous System Infection

Yumin Ding[1], Haiyu Wang[1], Kaixu Li[1], Shujing Zhao[1], Dehong Li[2]

[1]School of Public Health, Gansu University of Chinese Medicine, Lanzhou, Gansu, 730000, People's Republic of China; [2]Department of Blood Transfusion, Gansu Provincial Hospital, Lanzhou, Gansu, 730000, People's Republic of China

Correspondence: Dehong Li, Department of Blood Transfusion, Gansu Provincial Hospital, Lanzhou, Gansu, 730000, People's Republic of China, Tel +86-15117107318, Email ldh810109@126.com

Objective: Early diagnosis of central nervous system (CNS) infections remains challenging. The aim of this study was to explore and identify potential biomarkers of CNS infection by comparing cerebrospinal fluid (CSF) proteomic characteristics in patients with tuberculous meningitis (TBM), purulent meningitis (PM), and viral meningitis (VM), as well as in patients without CNS infections.

Methods: We conducted the first systematic 4D-DIA comparative proteomic analysis of CSF across TBM (N=6), PM (N=6), VM (N=12), and controls (N=12) using pooled samples. Differential proteins were identified, subjected to GO and KEGG enrichment analyses, and used to construct protein-protein interaction networks for hub protein identification.

Results: Proteomic analysis revealed significant differences in CSF protein expression profiles among three types of meningitis. In TBM patients, 53 specific proteins were identified, primarily involved in the complement and coagulation cascade as well as the COVID-19-related immune pathway. PPI network analysis highlighted FGA, FGB, C4BPA, and ADAMTS13 as hub proteins exhibiting notably significant expression levels in TBM patients. In PM patients, 9 proteins were identified, predominantly linked to phagosomes and B-cell receptor signaling, with COLEC11 and ESM1 showing significantly higher expression. In VM patients, 29 proteins were identified, mainly associated with complement and coagulation pathways, featuring higher levels of TMED7, MMP17, and CD81.

Conclusion: This study delineated the CSF protein profiles in patients with TBM, PM, VM, and non-CNS infections. We identified several potential biomarkers, including FGA, FGB, C4BPA, ADAMTS13, COLEC11, ESM1, TMED7, MMP17, and CD81. Additionally, we proposed hypothetical molecular mechanisms that may offer valuable diagnostic and therapeutic insights for CNS infections. Nonetheless, given that this is a preliminary exploratory study, further validation through multicenter, large-sample cohort studies and functional experiments is necessary to substantiate the clinical relevance and utility of these biomarkers prior to any potential application in clinical practice.

Keywords: cerebrospinal fluid, proteomics, central nervous system infection, early diagnosis, biomarkers

Introduction

Meningitis is a common central nervous system (CNS) infection, particularly prevalent in developing countries, and is characterized by high rates of infectivity, disability, and mortality. The World Health Organization estimates that about 250,000 individuals succumb to meningitis annually, with around 20% of survivors experiencing severe sequelae.[1] Thus, the early identification of the etiological agent, timely diagnosis, and selection of effective treatment strategies are crucial for improving patient prognosis and reducing mortality rates. The CNS infections mainly include viral meningitis (VM), purulent meningitis (PM), and tuberculous meningitis (TBM). Clinically, diagnosis and differentiation are primarily based on clinical signs, routine laboratory examinations, neuroimaging, and pathogen detection.[2] In the early stages of the disease, differentiating among these three distinct forms of meningitis through routine laboratory examination indicators and cranial imaging findings presents significant challenges, often resulting in potential misdiagnosis or

https://doi.org/10.2147/IDR.S570645
Received: 27 September 2025
Accepted: 20 January 2026
Published: 2 February 2026

missed diagnosis.[3–5] Concurrently, certain non-infectious neurological conditions, such as tension-type headaches and epilepsy, exhibit clinical manifestations that closely resemble those of CNS infections, including headache, vomiting, severe convulsions, and disturbances of consciousness.[6,7] This similarity complicates the diagnostic process. Although pathogen culture remains the gold standard for the clinical diagnosis of CNS infections, it is characterized by prolonged detection times and a low positive rate, which may result in missed optimal treatment opportunities.[8] In recent years, the widespread use of antibiotics in clinical practice has led to gradual reduction in the number of meningitis patients presenting with typical clinical manifestations and cerebrospinal fluid (CSF) examination findings. This trend has subsequently intensified the diagnostic challenges, complicating the accurate identification of different types of meningitis.[7] Therefore, finding diagnostic methods and indicators that possess high sensitivity and specificity is of great significance.

The use of a single biomarker presents limitations, including suboptimal sensitivity and low specificity, which hinder its ability to accurately diagnose CNS infections.[9] In contrast, proteomics offers a comprehensive approach by characterizing the expression of all proteins, post-translational modifications, interactions, and dynamic changes within a living organism.[10,11] Proteomics can provide comprehensive protein information involved in the pathogenesis, infection mechanism and pathological symptoms of the host, thereby providing a novel perspective for the screening, identification, and evaluation of biomarkers for CNS infections.[12] It is a useful tool in the research of infectious diseases. Previous studies have initially confirmed the application potential of proteomics in this field. For instance, Saima et al analyzed the CSF of patients with VM through proteomics and found that inflammation-related proteins such as S100A8 and S100A9 could serve as potential diagnostic markers.[13] Guadalupe et al explored the expression profile of inflammatory proteins in the CSF of patients with PM and discovered that proteins involved in immune response and exosome signaling were significantly enriched in infected samples.[14] In addition, Ghantasala et al found that amphoteric proteins (AMPH) and neurofascin proteins (NFASC) are closely related to TBM infection.[15] However, existing research is largely confined to analyses of single disease types, lacking systematic comparative studies across different CNS infections and non-infectious neurological controls. This gap limits the generalizability and practical application of proteomic biomarkers in the differential diagnosis of multiple clinical etiologies. Given these diagnostic dilemmas and the limitations of current research, there is an urgent clinical need to develop biomarker panels capable of early and accurate discrimination among CNS infection types.

This study employs advanced four-dimensional data-independent acquisition (4D-DIA) proteomics for high-throughput analysis. Building on traditional DIA, 4D-DIA incorporates ion mobility spectrometry as a fourth dimension of separation, combined with parallel accumulation–serial fragmentation (PASEF) technology.[16] This significantly enhances separation capability, detection sensitivity, and quantitative reproducibility for proteins in complex biological samples, making it particularly suitable for CSF studies characterized by low protein abundance, wide dynamic range, and limited sample availability.[17–20] This study aims to systematically analyze CSF samples from patients with TBM, PM, VM, and non-CNS infection controls using 4D-DIA technology, comprehensively comparing their differential protein profiles to identify characteristic protein combinations with diagnostic value. Upon successfully validated in subsequent studies, these potential biomarkers could become objective tools to assist clinical decision-making, optimizing current diagnostic workflows reliant on empirical judgment and time-consuming pathogen detection. This would improve the efficiency and accuracy of differential diagnosis, providing a critical basis for early intervention and personalized treatment of patients.

Materials and Methods

Patient Samples

Initially, fourteen patients were diagnosed with TBM, thirteen with PM, and sixty-three with VM. Additionally, fifty-two patients without CNS infections were recruited for this study. All participants were screened according to the pre-defined inclusion and exclusion criteria, which included specific etiological diagnostic requirements for each meningitis group (detailed in Supplementary Table 1). Finally, the study included a total of six patients with TBM as the TBM group, six patients with PM as the PM group, twelve patients with VM as the VM group, and

twelve age- and sex-matched non-CNS patients as the control group. The control group included neuropathic headache, trigeminal neuralgia, vertigo syndrome, and benign intracranial hypertension. These patients were clinically similar to those with CNS infections (exhibiting symptoms such as headache, vomiting, and others). However, after neurological physical examination, imaging examination, serological test and CSF analysis, the infectious cause was ruled out, and the final diagnosis was non-CNS disease. All patients included in this study were inpatients of the Department of Clinical Neurology, Gansu Provincial Hospital (Lanzhou, China). Demographic data along with clinical characteristics, diagnostic and laboratory findings were extracted from electronic medical records. The study protocol received approval from the Medical Ethics Committee of Gansu Provincial Hospital (No. 2024–308).

Collection and Preparation of CSF Sample

CSF samples were obtained by lumbar puncture within 24 to 72 hours of admission and prior to therapeutic intervention. Lumbar puncture was performed in strict accordance with clinical guidelines, and patients signed informed consent prior to sample collection. Routine cerebrospinal fluid (CSF) analysis in this study included the measurement of protein, chloride ion (Cl^-), white blood cell (WBC) count, red blood cell (RBC) count, adenosine deaminase (ADA) activity, glucose (Glu) concentration, immunoglobulin G (IgG) level, neutrophil percentage (NE%), and lymphocyte percentage (LY%). The assays were performed as follows: protein was determined using the pyrogallol red-molybdate method; Cl^- was measured by indirect ion-selective electrode potentiometry; WBC and RBC counts were obtained by manual microscopic enumeration; ADA activity was assessed by the peroxidase enzymatic assay; Glu concentration was quantified via the hexokinase enzymatic method; IgG level was analyzed by immunonephelometry; and NE% and LY % were determined by manual microscopic differential count. After clinical testing, the residual CSF sample was centrifuged at 1000 g at 4°C for 15 minutes to remove cellular debris. The supernatant was aliquoted into 1.5 mL Eppendorf tubes and stored at −80°C.

Sample Handling

To ensure the objectivity of the experiments and to minimize batch effects and technical bias, a randomization strategy was employed during the sample processing stage. The CSF samples from the TBM group (N=6), PM group (N=6), VM group (N=12), and control group (N=12) were randomly selected and mixed to create pooled samples. Specifically, samples from each group were mixed in equal volumes of 100 μL CSF, and each group was combined into three pooled samples, resulting in a total of 12 independent samples used for proteomic detection. The selection of individual samples for pooling and the subsequent sample processing workflow was carried out in a randomized order across the four diagnostic groups. The details of these patient samples are shown in Supplementary Table 2. Begin by retrieving the samples from the −80°C freezer and gently thawing them on ice. Then, add phenylmethylsulfonyl fluoride (PMSF) to the samples to achieve a final concentration of 1mM and thoroughly mix. Centrifuge at 4°C, 4500g for 10 minutes to collect the supernatant. Finally, determine the protein concentration using a BCA assay kit. If the sample concentration is too low (below 1 mg/mL), transfer the samples to 10KDa ultrafiltration tubes (Beckman Coulter Inc., Brea, CA), and repeat the ultrafiltration concentration process until the protein content meets the requirements. The main reagents and instruments required in this experiment are shown in Supplementary Tables 3 and 4.

Proteolytic Desalting

Start by taking 100μg of protein solution based on protein concentration, then adjust the volume to 200ul with 8M urea, followed by reduction with 5 mM dithiothreitol (DTT) at 37°C for 45 minutes, and alkylation with 11mM iodoacetamide (IAM) in a dark room at room temperature for 15 minutes. Then, add 800ul of 25mM ammonium bicarbonate solution and 3ul of Trypsin (Promega), and digest overnight at 37°C. Adjust the pH of the digested peptides to 2–3 using 20% trifluoroacetic acid (TFA), followed by desalting with C18 (Millipore, Billerica, MA) resin. Finally, determine the peptide concentration using a Pierce™ Quantitative Peptide Assay Kit with standards (Thermo Fisher).

LC-MS/MS Analysis

Liquid Chromatography Detection

Liquid chromatography (LC) was performed on a nanoElute UHPLC (Bruker Daltonics, Germany). About 200 ng of peptides were separated within 20 min at a flow rate of 0.5 μL/min on a commercially available reverse phase C18 column with an integrated CaptiveSpray Emitter (15cm75μm1.6μm, Aurora Series with CSI, IonOpticks, Australia). The separation temperature was kept by an integrated toaster column oven at 50 °C. Mobile phases A and B were produced with 0.1% formic acid in water and 0.1% formic acid in acetonitrile (ACN). Mobile phase B was increased from 5 to 25% over the first 17 min, increased to 40% over the next 1 min, further increased to 95% over the next 1 min, and then held at 95% for 1 min.

timsTOF Pro2 Mass Spectrometry Detection

To prevent any sequence-dependent bias, the 12 pooled samples were injected for LC-MS/MS analysis in a fully randomized order. The LC was coupled online to a hybrid timsTOF Pro2 (Bruker Daltonics, Germany) via a CaptiveSpray nano-electrospray ion source (CSI). To establish the applicable acquisition windows for DIA-PASEF mode, the timsTOF Pro2 was operated in Data-Dependent Parallel Accumulation-Serial Fragmentation (PASEF) mode with 4 PASEF MS/MS frames in 1 complete frame. The capillary voltage was set to 1500 V, and the MS and MS/MS spectra were acquired from 100 to 1700 m/z. As for ion mobility range ($1/K_0$), 0.85 to 1.3 Vs/cm^2 was used. The "target value" of 10,000 was applied to a repeated schedule, and the intensity threshold was set at 1500. The range of charge state was set from 0 to 5. The collision energy was ramped linearly as a function of mobility from 45eV at 1/ K_0 = 1.3 Vs/ cm^2 to 27 eV at 1/ K_0 = 0.85 Vs/ cm^2. The quadrupole isolation width was set to 2Th for m/z < 700 and 3Th for m/z > 800.

Database Search and Quantification

In this study, the DIA mass spectrometry data were processed using the DIA-NN (v1.8.1) search software with the Liberary-free method. The database used for searching was uniprot_proteomeUP000005640_human_20230504.fasta (containing 82,492 sequences), along with the iRT2.fasta database (containing 1 sequence) these was used to create a spectral library with deep learning algorithms of neural networks. The option of match between runs (MBR) was employed to create a spectral library from DIA data and then reanalyzed using this library. The false discovery rate (FDR) of the search results was adjusted to < 1% at both the protein and precursor ion levels, and the remaining identifications were used for further quantification analysis. To ensure an unbiased analytical process, all raw data files were anonymized with non-revealing sample codes prior to database searching and quantitative analysis. The investigator performing the bioinformatics analysis was blinded to the group assignments (TBM, PM, VM, Control) until the final list of differentially expressed proteins and their quantitative profiles were generated.

Bioinformatics Analysis

In this study, we used a variety of bioinformatics tools to dig deep into the proteomic data. First, the UniProt-GOA database was used to annotate all the screened proteins for gene ontology (GO) to identify their roles in different biological processes, cellular components, and molecular functions. Secondly, pathway enrichment analysis was performed using the Kyoto Encyclopedia of Genes and Genomes (KEGG) database to identify key metabolic and signal transduction pathways involved in differentially expressed proteins. In addition, the protein-protein interaction (PPI) network was constructed using the online STRING tool to explore the relationships among these differentially expressed proteins and to identify key proteins that may play an important role in the pathological process of meningitis.

Statistical Analysis

Statistical analyses were conducted using SPSS 24.0. Quantitative variables were reported as mean ± standard deviation (SD) or as median and interquartile range, while categorical variables were expressed as percentages (%). When continuous variable data adhere to a normal distribution, an independent samples *t*-test was employed for comparisons between two groups, while a one-way analysis of variance (ANOVA) was utilized for comparisons among multiple groups. Conversely, when continuous variable data deviate from a normal distribution, the Kruskal–Wallis H (K) test was

used for comparisons among multiple groups, and the Mann–Whitney *U*-test was applied for comparisons between two groups. Categorical variables were compared using the chi-square test. $P < 0.05$ was considered statistically significant.

Results

Basic Characteristics of the Participants

In this study, we divided the participants into four groups: Control group (N=12), TBM group (N=6), PM group (N=6) and VM group (N=12). The basic demographic characteristics and clinical data for these groups are shown in Table 1. No significant statistical difference was observed among the four groups with respect to age (P=0.912) and gender distribution (P=0.801). Specifically, the mean ages were 38.58±3.48 years for the control group, 35.83±5.81 years for the TBM group, 39.00±12.12 years for the PM group, and 35.50±3.89 years for the VM group. The gender distributions were as follows: 41.7% male and 58.3% female in the control group, 50% male and 50% female in the TBM group, 66.7% male and 33.3% female accounted for in the PM group, and 50% male and 50% female in the VM group. CSF analysis revealed the following findings. First, the WBC count, RBC count, IgG levels, NE%, and LY% were significantly elevated in the TBM, PM, and VM groups compared to the control group ($P < 0.05$). However, no statistically significant differences were observed among the TBM, PM, and VM groups with respect to these parameters. Secondly, compared with the control group, the ADA levels in the TBM group and the VM group increased, and the difference was statistically significant ($P < 0.05$). However, there was no significant difference in ADA levels between the control group and the PM group ($P > 0.05$), and there were also no significant differences in pairwise comparisons among the TBM, PM, and VM groups ($P > 0.05$). Finally, compared with the control group, the protein levels in the CSF of the PM group and the VM group were higher, with statistically significant differences ($P < 0.05$). However, there was no significant difference in protein levels in CSF between the control group and the TBM group ($P > 0.05$), and pairwise comparisons among the TBM, PM, and VM groups also showed no significant differences ($P > 0.05$).

Quality Control of Proteomics Data

To explore the proteomic patterns in the CSF of CNS infections, we performed proteomic analyses on three groups of meningitis and a control group. Protein identification and quantification were robust, with a total of 5854 proteins reliably detected across the samples (Supplementary Figure 1A). This ensures that the dataset was both comprehensive and

Table 1 Baseline Characteristics of the Patients

	Control N=12	TBM N=6	PM N=6	VM N=12	*P*	CSF Test Method
Basic profile						
Age	38.58±3.48	35.83±5.81	39.00±12.12	35.50±3.89	0.912	
Gender					0.801	
Male	5(41.7%)	3(50.0%)	4(66.7%)	6(50.0%)		
Female	7(58.3%)	3(50.0%)	2(33.3%)	6(50.0%)		
CSF test						
Cl^- (mmol/L)	112.78(122.07–124.85)	122.61(115.07–125.49)	115.83±8.43	122.31±3.62	0.308	Ion-selective electrode method
WBC (10^9/L)	1.00(0.00–1.00)	193.00±235.37[a]	395.00(1.75–2417.75)[b]	60.50(12.00–101.25)[c]	0.000	Microscope count method
RBC (10^{12}/L)	0.00	8.00(0.00–292.75)[a]	20.00(0.00–433.75)[b]	3.00(0.00–129.75)[c]	0.033	Microscope count method
ADA (U/L)	0.20(0.09–0.28)	1.59(0.31–7.42)[a]	1.67±1.72	0.47(0.25–1.17)[c]	0.014	Peroxidase method
Protein (g/L)	0.30±0.04	1.43±1.47	1.13(0.31–1.90)[b]	0.42±0.14[c]	0.005	Pyrogallol Red-molybdate method
Glu (mmol/L)	3.26(3.04–3.67)	2.96±0.68	2.85±1.44	3.14±0.48	0.696	Hexokinase method
IgG (mg/L)	29.13±6.63	103.50(32.30–426.50)[a]	127.35±88.32[b]	52.34±26.12[c]	0.016	Immunoturbidimetry
NE (%)	0.00	4.00(0.00–15.25)[a]	2.50(0.00–45.5)[b]	1.50(0.00–4.00)[c]	0.008	Microscope count method
LY (%)	0.00	46.00(0.00–94.50)[a]	62.83±45.04[b]	96.00(11.25–98.75)[c]	0.002	Microscope count method

Notes: [a]Control group vs TBM group, $P < 0.05$; [b]Control group vs PM group, $P < 0.05$; [c]Control group vs VM group, $P < 0.05$.
Abbreviations: WBC, White Blood Cell count; RBC, Red Blood Cell count; ADA, Adenosine Deaminase; Glu, Glucose; IgG, Immunoglobulin G; NE, Neutrophil Percentage; LY, Lymphocyte Percentage.

https://doi.org/10.2147/IDR.S570645

representative, facilitating subsequent analytical endeavors. Violin plot analysis demonstrated the distribution of protein expression levels within each sample, showing concentrated data fluctuations that indicate low variability and high reproducibility among samples (Supplementary Figure 1B). Correlogram analysis revealed that samples within the same group exhibited higher correlation coefficients, while samples from different groups demonstrated lower correlation coefficients. This observation indicates that the overall stability of the detection process is robust and the data quality is high (Supplementary Figure 1C). Together, these analyses verified the robustness and reliability of the dataset, providing strong support for further investigation into the differences in protein expression among the three types of meningitis.

Selection of Specifically Expressed Proteins in Three Types of Meningitis

Proteins exhibiting significant differences between each pair of groups were selected based on the criteria of fold change (FC) ≥ 1.5 or FC ≤ 0.6667 and P-value ≤ 0.05.

Our study delineates the unique proteomic profile of the TBM group relative to the other cohorts. The results showed that compared to the control group, 1646 proteins were upregulated and 530 were downregulated in the TBM group (Figure 1A); Compared to the PM group, 410 proteins were upregulated and 598 were downregulated in the TBM group (Figure 1B); Compared to the VM group, 88 proteins were upregulated and 2112 were downregulated in the TBM group (Figure 1C). To identify proteins specifically expressed in TBM, we further screened overlapping proteins that could be detected in TBM, PM, VM, and control groups (Supplementary Table 5). Ultimately, compared with the PM, VM, and control groups simultaneously, we screened 53 overlapping proteins that were specifically expressed in the TBM group (Table 2).

Additionally, our study provides a comprehensive analysis of the proteomic characteristics of the PM group in comparison with the other groups. The results showed that compared to the control group, 1328 proteins were upregulated and 139 were downregulated in the PM group (Figure 1D); Compared to the TBM group, 598 proteins were upregulated and 410 were downregulated in the PM group (Figure 1E); Compared to the VM group, 69 proteins were upregulated and 1910 were downregulated in the PM group (Figure 1F). To identify proteins specifically expressed in PM, we further screened overlapping proteins that could be detected in PM, TBM, VM, and control groups (Supplementary Table 5). Ultimately, compared with the TBM, VM, and control groups simultaneously, we screened 9 overlapping proteins that were specifically expressed in the PM group (Table 3).

Lastly, our study encapsulates the proteomic profile of the VM group in relation to the other groups. The results showed that compared to the control group, 3199 proteins were upregulated and 56 were downregulated in the VM group (Figure 1G); Compared to the TBM group, 2112 proteins were upregulated and 88 were downregulated in the VM group (Figure 1H); Compared to the PM group, 1910 proteins were upregulated and 69 were downregulated in the VM group (Figure 1I). To identify proteins specifically expressed in VM, we further screened overlapping proteins that could be detected in VM, TBM, PM, and control groups (Supplementary Table 5). Ultimately, compared with the TBM, PM, and control groups simultaneously, we screened 29 overlapping proteins that were specifically expressed in the VM group (Table 4).

Bioinformatics Analysis and Identification of Specific Proteins in Three Types of Meningitis

In order to further explore the functions and expression patterns of the overlapping specifically expressed proteins in the three types of meningitis, we conducted a comprehensive bioinformatics analysis of 53 overlapping proteins specifically expressed in the TBM group, 9 overlapping proteins specifically expressed in the PM group, and 29 overlapping proteins specifically expressed in the VM group.

Gene Ontology Enrichment Analysis

Gene Ontology (GO) analysis (Figure 2A–C) showed that, in terms of biological processes, the specifically expressed proteins in both the TBM and VM groups were primarily involved in mediating the innate immune response (GO:0045087) and the classical pathway of complement activation (GO:0006958). In contrast, the specifically expressed proteins in the PM group were predominantly associated with the defense response to bacterium (GO:0042742), positive regulation of B cell activation (GO:0050871), and proteolysis (GO:0006508). In addition, in the TBM group, the cellular

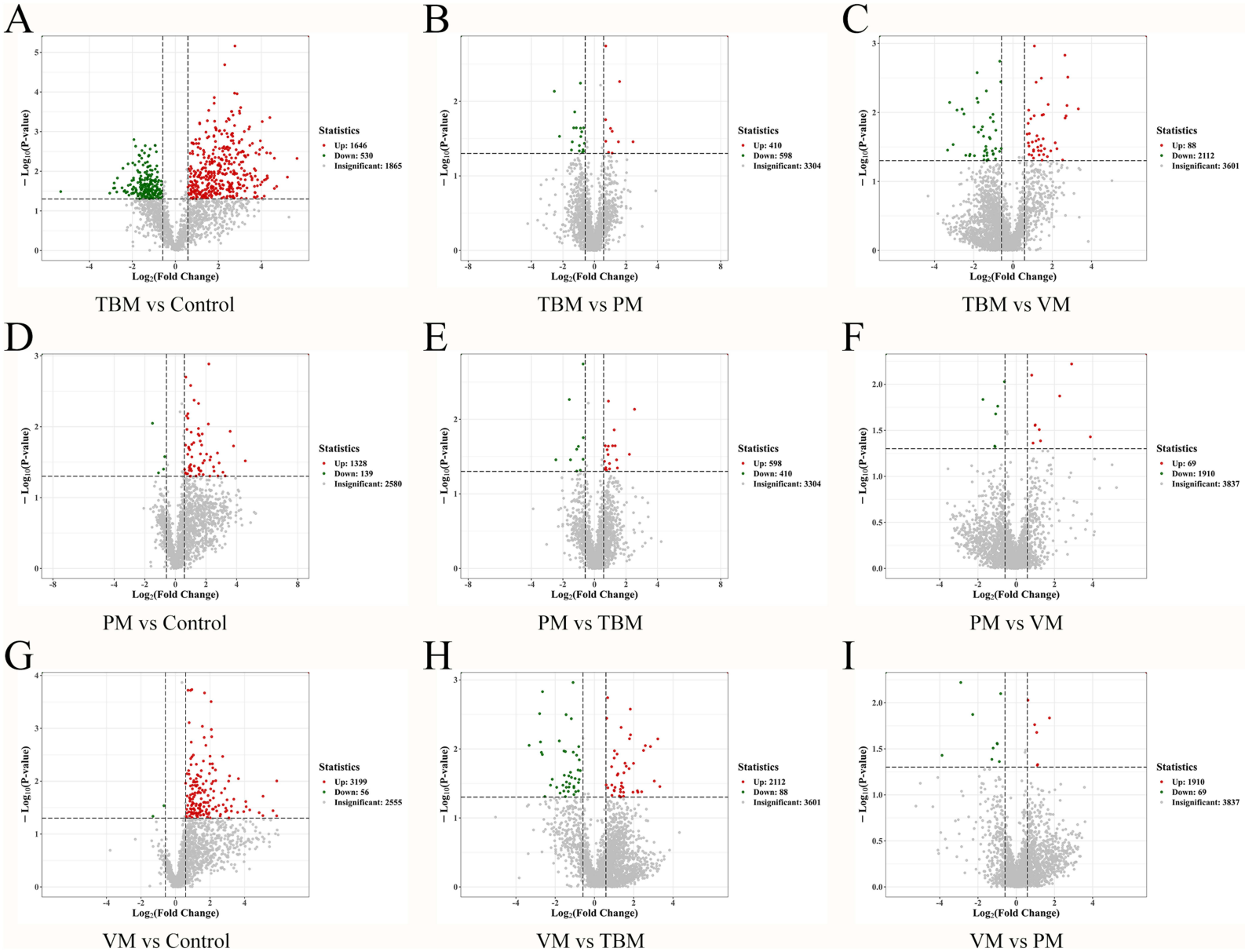

Figure 1 The specifically expressed proteins analyzed by volcano plots between every two groups. (**A**) TBM group vs Control group. (**B**) TBM group vs PM Group. (**C**) TBM group vs VM group. (**D**) PM group vs Control group. (**E**) PM group vs TBM group. (**F**) PM group vs VM group. (**G**) VM group vs Control group. (**H**) VM group vs TBM group. (**I**) VM group vs PM group.

https://doi.org/10.2147/IDR.S570645

https://doi.org/10.2147/IDR.S570645

Table 2 Specifically Expressed Proteins in TBM Group

Gene Name	Abundances												TBM vs Control		TBM vs PM		TBM vs VM	
	TBM			PM			VM			Control			Ratio	*P*	Ratio	*P*	Ratio	*P*
IGLC7	1173.22	1538.40	2392.80	1405.16	180.38	1361.47	832.00	538.11	390.95	268.12	206.95	187.95	7.70	0.003	1.73	0.341	2.90	0.024
IGHG3	1009.38	890.32	1003.36	699.09	171.25	937.79	486.86	346.13	247.13	251.41	103.76	176.87	5.46	0.019	1.61	0.316	2.69	0.030
IGHA1	553.97	444.80	403.82	430.58	110.58	427.40	214.11	161.78	302.65	115.15	77.38	157.46	4.01	0.010	1.45	0.362	2.07	0.035
FGB	466.01	414.12	315.39	245.29	28.49	207.32	163.76	117.29	158.08	33.55	32.45	33.71	11.99	<0.001	2.490	0.003	2.72	0.002
ITIH4	180.67	169.94	152.78	188.29	34.81	148.56	107.44	60.92	75.40	46.88	46.21	48.84	3.55	0.001	1.35	0.425	2.07	0.036
APOH	160.47	137.91	146.05	137.99	38.20	177.71	105.67	75.54	88.38	49.25	49.62	52.58	2.93	<0.001	1.26	0.477	1.65	0.021
IGLV1-51	151.22	76.03	224.80	81.26	7.77	88.03	57.11	23.17	15.59	26.54	5.79	5.91	11.82	0.016	2.55	0.245	4.72	0.034
FGA	137.88	171.92	128.62	100.18	24.80	71.35	88.83	78.99	88.82	16.37	21.52	22.08	7.31	<0.001	2.23	0.008	1.71	0.014
MACF1	90.69	34.53	76.79	59.26	3.13	25.85	10.19	16.18	5.71	3.32	2.33	2.65	24.35	0.005	2.29	0.272	6.30	0.012
IGLV8-61	83.16	46.70	55.84	18.73	1.96	37.64	11.49	7.65	10.54	11.35	5.82	6.42	7.87	0.002	3.18	0.196	6.26	0.001
ITIH2	75.94	82.63	86.87	84.18	17.50	51.72	46.90	36.95	55.86	22.12	17.49	30.18	3.52	0.011	1.60	0.293	1.76	0.031
JCHAIN	73.99	53.96	63.58	47.46	6.77	33.69	21.98	12.66	20.73	8.12	10.60	9.68	6.75	<0.001	2.18	0.220	3.46	0.008
PON3	73.06	91.24	80.91	70.13	17.56	113.38	48.77	30.34	44.97	22.92	20.86	26.45	3.49	<0.001	1.22	0.506	1.98	0.027
SAA4	61.91	87.94	65.56	96.43	11.69	78.98	43.92	32.23	38.66	14.89	11.81	12.35	5.52	<0.001	1.15	0.564	1.88	0.012
IGHV1-18	43.41	17.49	46.43	15.94	0.00	21.80	11.89	4.90	1.83	4.68	0.63	1.26	16.34	0.019	1.90	0.214	5.77	0.049
C4BPA	36.55	65.35	54.65	20.45	3.56	24.62	29.89	16.62	16.84	2.62	3.22	3.68	16.45	0.001	3.18	0.006	2.470	0.025
IGHV1-3	18.28	16.23	45.40	24.96	0.98	24.59	7.98	6.51	3.51	5.84	2.43	1.44	8.24	0.016	1.58	0.441	4.44	0.028
IGLV7-46	15.77	33.36	25.30	15.22	1.42	14.28	5.13	3.05	2.57	6.87	0.95	1.02	8.42	0.048	2.41	0.245	6.93	0.003
APOF	14.42	12.80	12.60	11.66	1.59	9.29	6.94	5.57	6.20	1.88	1.83	2.12	6.83	<0.001	1.77	0.302	2.13	0.001
PNO1	12.34	13.41	10.17	9.21	5.22	9.35	8.15	4.95	7.26	4.46	6.36	7.05	2.01	0.018	1.51	0.135	1.76	0.041
CFHR1	10.62	15.06	15.52	14.43	4.12	14.35	8.90	6.72	8.39	3.58	3.86	6.07	3.05	0.007	1.25	0.488	1.72	0.028
NDUFV1	7.05	5.88	8.29	4.22	0.00	2.08	3.41	1.87	3.57	0.90	1.27	1.27	6.17	<0.001	2.25	0.229	2.40	0.032
IGHV1-8	6.85	2.58	2.89	0.77	0.00	0.74	0.53	0.36	0.34	0.46	0.00	0.27	11.11	0.011	5.45	0.035	10.04	0.009
OMD	6.53	8.56	4.52	5.62	30.21	9.14	20.55	17.65	29.37	19.03	17.56	20.54	0.34	0.022	0.44	0.352	0.29	0.007
CRISP3	6.03	7.62	5.04	19.32	0.82	6.29	3.43	2.05	1.44	1.00	0.71	0.66	7.88	<0.001	0.71	0.790	2.70	0.036
RNASE6	5.20	5.75	5.20	4.09	4.21	3.22	2.55	1.10	1.82	1.34	2.54	1.19	3.18	0.033	1.40	0.042	2.95	0.041
VWF	4.86	4.94	4.20	9.55	2.05	3.92	2.99	2.08	2.79	1.28	1.21	1.50	3.51	<0.001	0.90	0.860	1.78	0.020
ADAMTS13	4.11	3.95	3.19	1.23	0.51	2.86	1.03	1.23	1.78	1.18	1.02	0.82	3.73	0.001	2.45	0.004	2.79	0.003
PIANP	3.33	5.27	0.00	0.00	37.18	15.30	47.11	12.98	46.70	29.60	35.21	42.12	0.12	0.036	0.16	0.109	0.12	0.029
PI16	3.02	3.56	2.91	6.21	7.50	3.60	7.52	5.00	10.37	8.71	5.26	7.38	0.44	0.021	0.55	0.117	0.41	0.048
C4BPB	2.65	3.02	2.83	2.91	0.17	1.55	1.25	0.58	0.97	0.16	0.06	0.22	19.30	0.013	1.84	0.320	3.04	0.034
VAT1	1.75	1.74	1.29	2.00	0.53	1.82	0.69	0.81	0.62	0.46	0.46	0.50	3.37	0.004	1.10	0.638	2.26	0.004
CFHR5	1.59	1.12	1.94	1.92	0.41	0.70	0.70	0.49	0.88	0.00	0.43	0.46	3.46	0.015	1.54	0.307	2.25	0.026
FKBP2	1.44	1.62	0.00	0.83	0.81	0.00	0.83	0.81	1.01	0.81	1.00	0.96	1.66	0.011	1.86	0.048	1.74	0.009

TNC	1.09	2.11	1.62	1.34	0.80	0.89	0.91	0.60	0.83	0.41	0.58	0.60	3.03	0.013	1.59	0.145	2.06	0.046
FSTL3	0.85	0.45	0.54	0.93	1.98	2.15	1.79	0.99	2.26	0.81	1.06	1.08	0.63	0.105	0.36	0.045	0.37	0.036
DNASE2	0.81	0.92	0.00	0.20	1.73	0.77	1.93	1.41	1.91	2.79	2.56	3.00	0.31	0.004	0.96	0.694	0.49	0.011
SLC12A5	0.76	1.01	0.70	1.20	1.45	0.00	1.44	0.32	2.76	1.19	1.39	1.84	0.56	0.027	0.62	0.047	0.55	0.702
NSF	0.68	1.10	0.81	0.71	2.02	0.90	1.81	1.98	2.01	1.62	1.37	2.08	0.51	0.024	0.71	0.513	0.45	0.024
SUMF2	0.65	0.77	0.86	0.55	1.59	0.97	1.12	0.97	1.36	0.95	1.32	1.34	0.63	0.036	0.73	0.540	0.66	0.033
CAMK2B	0.64	1.38	1.06	0.66	2.80	0.75	2.61	2.32	3.78	1.74	2.99	2.59	0.42	0.038	0.73	0.814	0.35	0.022
GRIA4	0.60	1.87	0.96	0.23	12.89	1.05	4.18	2.50	8.94	5.44	8.86	7.88	0.15	0.015	0.24	0.795	0.22	0.040
TMED7	0.49	0.57	0.51	0.78	1.21	0.56	1.48	2.08	2.00	0.87	1.00	1.38	0.48	0.025	0.61	0.178	0.28	0.003
KRT19	0.48	0.76	0.72	0.27	0.00	0.68	1.47	0.00	2.17	1.27	2.92	1.76	0.33	0.028	1.38	0.542	0.36	0.049
CPAMD8	0.33	0.30	0.00	0.76	0.79	0.00	0.76	0.68	0.96	0.69	0.80	0.75	0.42	0.004	0.40	0.023	0.39	0.005
GALNT11	0.28	0.00	0.21	0.00	0.41	0.00	0.56	0.00	0.71	0.39	0.73	0.61	0.42	0.036	0.59	<0.001	0.39	0.034
TOLLIP	0.22	0.22	0.00	0.41	0.58	0.77	0.87	0.63	1.16	0.64	0.32	0.58	0.44	0.069	0.38	0.035	0.25	0.016
NPC1	0.13	0.20	0.00	0.00	1.56	0.32	0.77	1.31	1.55	0.98	0.00	1.44	0.14	0.020	0.18	0.304	0.14	0.009
ECRG4	0.13	0.00	0.18	0.41	1.83	0.00	0.91	0.72	1.14	0.64	0.65	1.95	0.14	0.026	0.14	0.246	0.17	0.009
ARSG	0.00	0.17	0.15	0.22	0.66	0.00	0.52	0.00	0.60	0.54	0.32	0.27	0.42	0.046	0.36	0.354	0.28	0.006
RCN2	0.00	0.29	0.22	0.00	1.03	0.38	0.67	0.57	1.02	0.70	0.87	0.73	0.33	0.029	0.36	0.305	0.34	0.016
SLC12A2	0.00	0.30	0.32	0.45	0.65	0.53	0.59	0.22	0.89	0.77	0.73	0.60	0.44	0.003	0.57	0.026	0.55	0.379
COL5A1	0.00	0.36	0.42	0.00	0.76	0.67	0.66	0.00	0.78	0.28	0.48	0.38	1.02	0.814	0.54	0.023	0.54	0.033

https://doi.org/10.2147/IDR.S570645

Table 3 Specifically Expressed Proteins in PM Group

Gene Name	Abundances												PM vs Control		PM vs TBM		PM vs VM	
	PM			TBM			VM			Control			Ratio	*P*	Ratio	*P*	Ratio	*P*
COLEC11	2.16	1.36	1.68	0.52	0.87	0.79	0.29	0.56	1.04	0.78	0.88	1.05	1.91	0.021	2.38	0.002	2.75	0.003
STAB1	2.01	2.10	2.37	1.09	1.47	1.46	2.17	1.13	2.32	0.85	1.24	1.08	2.05	0.012	1.61	0.023	1.15	0.502
ADAM28	1.13	0.81	0.64	0.44	0.57	0.32	0.62	0.52	0.97	0.33	0.45	0.44	2.11	0.027	1.94	0.046	1.23	0.441
ESM1	0.92	0.60	0.64	0.36	0.38	0.00	0.20	0.45	0.28	0.44	0.23	0.37	2.07	0.042	1.94	0.039	2.32	0.040
PLBD1	0.92	0.00	0.95	0.78	1.07	0.00	0.48	0.59	0.53	0.32	0.34	0.20	3.29	0.018	1.01	0.920	1.76	0.008
IGHV1-8	0.77	0.00	0.74	6.85	2.58	2.89	0.53	0.36	0.34	0.46	0.00	0.27	2.04	0.214	0.18	0.035	1.84	0.044
CD81	0.68	0.76	0.61	0.92	0.64	0.00	0.00	1.44	1.23	0.46	0.29	0.27	2.00	0.039	0.78	0.579	0.51	0.017
MYL11	0.00	6.77	7.11	0.71	13.77	4.62	4.33	3.38	2.79	1.46	1.76	1.35	4.56	0.001	1.09	0.522	1.98	0.028
COL5A1	0.00	0.76	0.67	0.00	0.36	0.42	0.66	0.00	0.78	0.28	0.48	0.38	1.88	0.041	1.84	0.023	1.00	0.982

https://doi.org/10.2147/IDR.S570645

Table 4 Specifically Expressed Proteins in VM Group

Gene Name	Abundances												VM vs Control		VM vs TBM		VM vs PM	
	VM			TBM			PM			Control			Ratio	*P*	Ratio	*P*	Ratio	*P*
IGLC7	832.00	538.11	390.95	1173.22	1538.40	2392.80	1405.16	180.38	1361.47	268.12	206.95	187.95	2.66	0.033	0.35	0.024	0.60	0.777
FGB	163.76	117.29	158.08	466.01	414.12	315.39	245.29	28.49	207.32	33.55	32.45	33.71	4.40	0.005	0.37	0.002	0.91	0.814
IGHM	123.85	113.75	41.86	212.94	408.79	439.18	397.13	10.49	220.61	26.78	8.42	20.58	5.01	0.031	0.26	0.036	0.44	0.910
APOH	105.67	75.54	88.38	160.47	137.91	146.05	137.99	38.20	177.71	49.25	49.62	52.58	1.78	0.024	0.61	0.021	0.76	0.862
FGA	88.83	78.99	88.82	137.88	171.92	128.62	100.18	24.80	71.35	16.37	21.52	22.08	4.28	0.001	0.59	0.014	1.31	0.513
PON3	48.77	30.34	44.97	73.06	91.24	80.91	70.13	17.56	113.38	22.92	20.86	26.45	1.77	0.045	0.51	0.027	0.62	0.706
ITIH2	46.90	36.95	55.86	75.94	82.63	86.87	84.18	17.50	51.72	22.12	17.49	30.18	2.00	0.027	0.57	0.031	0.91	0.881
SAA4	43.92	32.23	38.66	61.91	87.94	65.56	96.43	11.69	78.98	14.89	11.81	12.35	2.94	0.001	0.53	0.012	0.61	0.833
MGP	32.68	45.17	50.76	23.76	15.38	18.68	23.82	41.02	19.46	14.19	23.03	18.78	2.30	0.012	2.22	0.012	1.53	0.168
C4BPA	29.89	16.62	16.84	36.55	65.35	54.65	20.45	3.56	24.62	2.62	3.22	3.68	6.66	0.003	0.40	0.025	1.30	0.827
JCHAIN	21.98	12.66	20.73	73.99	53.96	63.58	47.46	6.77	33.69	8.12	10.60	9.68	1.95	0.049	0.29	0.008	0.63	0.765
MACF1	10.19	16.18	5.71	90.69	34.53	76.79	59.26	3.13	25.85	3.32	2.33	2.65	3.87	0.040	0.16	0.012	0.36	0.607
CFHR1	8.90	6.72	8.39	10.62	15.06	15.52	14.43	4.12	14.35	3.58	3.86	6.07	1.78	0.048	0.58	0.028	0.73	0.715
APOF	6.94	5.57	6.20	14.42	12.80	12.60	11.66	1.59	9.29	1.88	1.83	2.12	3.21	<0.001	0.47	0.001	0.83	0.878
MYL11	4.33	3.38	2.79	0.71	13.77	4.62	0.00	6.77	7.11	1.46	1.76	1.35	2.30	0.009	0.55	0.973	0.50	0.028
CRISP3	3.43	2.05	1.44	6.03	7.62	5.04	19.32	0.82	6.29	1.00	0.71	0.66	2.92	0.037	0.37	0.036	0.26	0.501
NDUFV1	3.41	1.87	3.57	7.05	5.88	8.29	4.22	0.00	2.08	0.90	1.27	1.27	2.58	0.028	0.42	0.032	0.94	0.928
HPRT1	3.26	3.00	3.50	2.16	2.28	1.90	1.73	2.59	3.09	1.79	1.92	2.41	1.60	0.019	1.54	0.004	1.32	0.216
RAD23B	3.10	3.02	2.89	1.47	1.95	1.49	1.50	2.42	2.50	1.61	2.31	1.91	1.54	0.046	1.83	0.018	1.40	0.157
VWF	2.99	2.08	2.79	4.86	4.94	4.20	9.55	2.05	3.92	1.28	1.21	1.50	1.97	0.012	0.56	0.020	0.51	0.381
DNASE2	1.93	1.41	1.91	0.81	0.92	0.00	0.20	1.73	0.77	2.79	2.56	3.00	0.63	0.029	2.03	0.011	1.94	0.255
SF3A1	1.58	1.45	1.41	0.60	0.83	0.79	0.68	1.17	0.64	0.84	0.76	0.82	1.83	<0.001	2.01	0.014	1.78	0.082
TMED7	1.48	2.08	2.00	0.49	0.57	0.51	0.78	1.21	0.56	0.87	1.00	1.38	1.71	0.038	3.55	0.003	2.18	0.047
C4BPB	1.25	0.58	0.97	2.65	3.02	2.83	2.91	0.17	1.55	0.16	0.06	0.22	6.34	0.017	0.33	0.034	0.60	0.971
MMP17	0.89	0.20	0.87	0.20	0.54	0.56	0.47	0.60	0.20	0.53	0.52	0.55	1.65	0.046	1.51	0.041	1.54	0.040
COL5A1	0.66	0.00	0.78	0.00	0.36	0.42	0.00	0.76	0.67	0.28	0.48	0.38	1.89	0.038	1.85	0.033	1.00	0.982
IGHV1-8	0.53	0.36	0.34	6.85	2.58	2.89	0.77	0.00	0.74	0.46	0.00	0.27	1.11	0.744	0.10	0.009	0.54	0.044
PLBD1	0.48	0.59	0.53	0.78	1.07	0.00	0.92	0.00	0.95	0.32	0.34	0.20	1.87	0.049	0.57	0.141	0.57	0.008
CD81	0.00	1.44	1.23	0.92	0.64	0.00	0.68	0.76	0.61	0.46	0.29	0.27	3.91	0.007	1.71	0.015	1.95	0.017

https://doi.org/10.2147/IDR.S570645

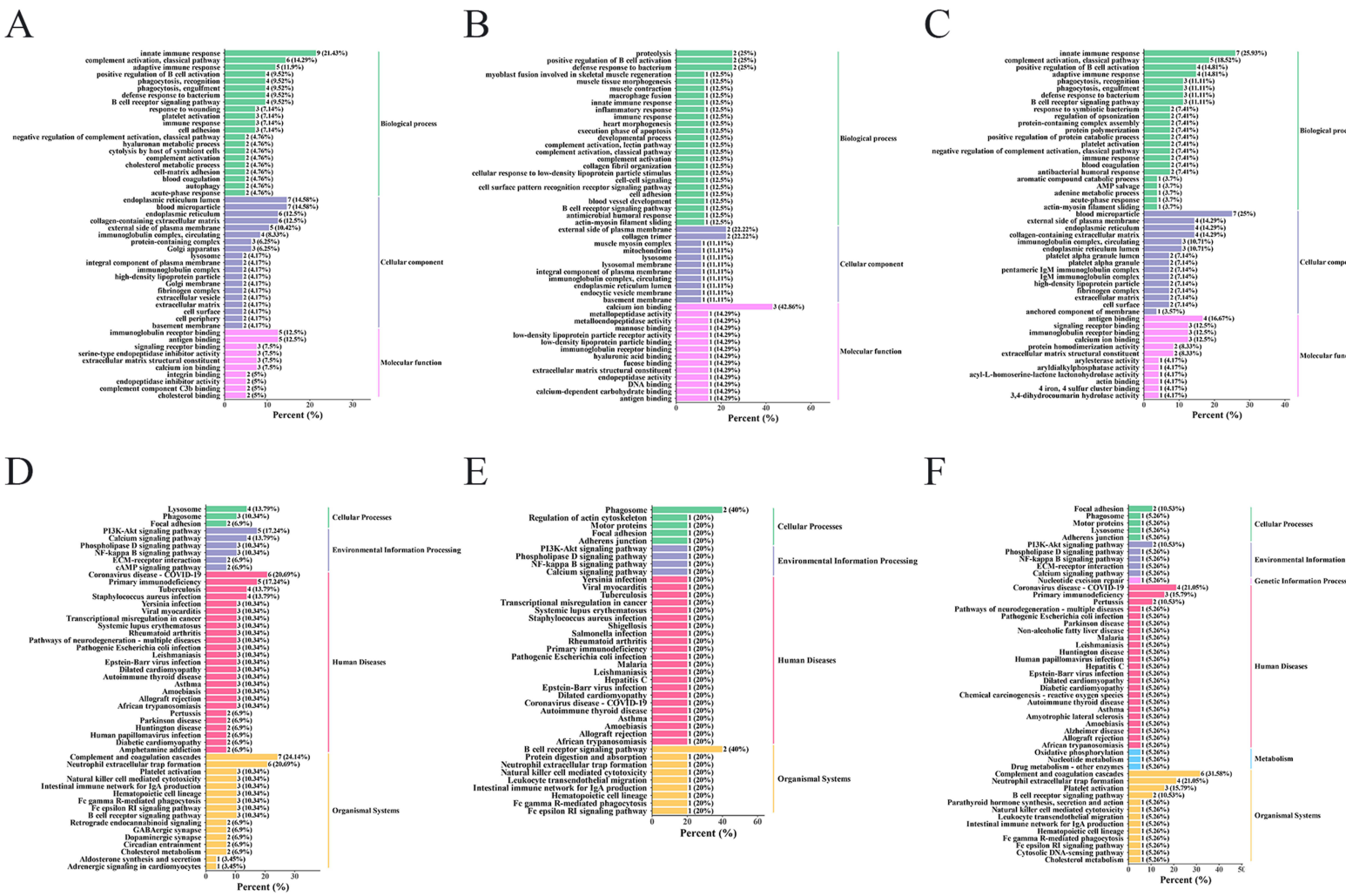

Figure 2 The function analysis of the specifically expressed proteins in three groups of meningitis. (**A**) GO analysis of the specifically expressed proteins in TBM group. (**B**) GO analysis of the specifically expressed proteins in PM group. (**C**) GO analysis of the specifically expressed proteins in VM group. (**D**) KEGG pathway analysis of the specifically expressed proteins in TBM group. (**E**) KEGG pathway analysis of the specifically expressed proteins in PM group. (**F**) KEGG pathway analysis of the specifically expressed proteins in VM group.

components most significantly enriched in specifically expressed proteins were blood microparticles (GO:0072562) and the endoplasmic reticulum lumen (GO:0005788). In the PM group, the cellular components most significantly enriched were collagen trimers (GO:0005581) and the external side of the plasma membrane (GO:0009897). The most significantly enriched cellular component in the VM group was blood microparticles (GO:0072562). In terms of molecular functions, the most significantly enriched molecular functions of specifically expressed proteins in the TBM group were immunoglobulin receptor binding (GO:0034987) and antigen binding (GO:0003823). In the PM group, the most significantly enriched molecular function was calcium ion binding (GO:0005509). The most significantly enriched molecular function in the VM group is antigen binding (GO:0003823).

Kyoto Encyclopedia of Genes and Genomes Pathway Enrichment Analysis

Kyoto Encyclopedia of Genes and Genomes (KEGG) pathway analysis further revealed the distinct roles played by the specifically expressed proteins associated with the three types of meningitis in immune responses and other biological processes.

The KEGG database analysis (Figure 2D–F) showed that the proteins in the TBM group were significantly enriched in the immune pathways. Notably, these include complement and coagulation cascade (ko04610) and Coronavirus disease-COVID-19 (ko05171). Proteins specifically associated with the complement and coagulation cascade include FGB, FGA, CFHR1, VWF, C4BPB, and CFHR5. The specific proteins associated with COVID-19 were FGB, FGA, IGHV1-18, IGHV1-3, and IGHV1-8. In the PM group, significant enrichment was observed in phagosomes (ko04145) and B-cell receptor signaling pathways (ko04662). The specific proteins associated with phagosomes were IGHV1-8 and COLEC11. The specific proteins associated with the B-cell receptor signaling pathway were IGHV1-8 and CD81. For the VM group, significant enrichment was noted in the complement and blood coagulation cascade (ko04610). The specific proteins related to the pathway were FGB, FGA, C4BPA, CFHR1, VWF, and C4BPB.

Protein-Protein Interaction (PPI) Network Analysis

Through GO and KEGG enrichment analysis, we gained an initial understanding of the classification of specifically expressed proteins. To further understand the interactions between specifically expressed proteins, the STRING tool was used to construct protein-protein interaction (PPI) network maps for the specific proteins screened in the three groups of meningitis. The PPI network was then visualized using Cytoscape software. One of the important ways proteins functions is by interacting with other proteins, exerting biological regulation through interprotein-mediated pathways, or forming complexes, in which proteins with high connectivity may be key sites in the entire signal transduction pathway. Therefore, we focused on proteins with higher connectivity levels, ie, those with node degrees ≥10, because they may have a more important role.[21]

Our results showed that the hub proteins identified in the TBM group included FGA, APOH, FGB, ITIH2, C4BPA, ITIH4, and ADAMTS13 (Figures 3A and B). Similarly, we utilized the STRING tool to construct a PPI network diagram for 9 specific proteins in the PM group (Figure 3C). However, due to the limited number of specific proteins identified in the PM group, the PPI network exhibited no nodal connections among the proteins. In the VM group, our results showed that the hub proteins identified included APOH, FGA, FGB, C4BPB, C4BPA, and ITIH2 (Figure 3D and E).

Comparative Analysis of Specific Proteins in Three Types of Meningitis

By comparing the specifically expressed proteins of all groups, we found that the expression levels of FGA, FGB, C4BPA, ADAMTS13, and other proteins in the TBM group were significantly higher than those in the other three groups. The expression levels of COLEC11 and ESM1 in the PM group were also higher than those in the other three groups. Similarly, the expression levels of TMED7, MMP17, and CD81 in the VM group were significantly higher than those in the other groups (Table 5 and Figure 4). To assess the differentiation potential of proteins such as FGA, FGB, C4BPA, ADAMTS13, COLEC11, ESM1, TMED7, MMP17 and CD81 among different groups, we plotted Receiver operator characteristic (ROC) curve and heat maps of protein correlations. The specificity and correlation of 9 proteins in TBM group, PM group and VM group were analyzed.

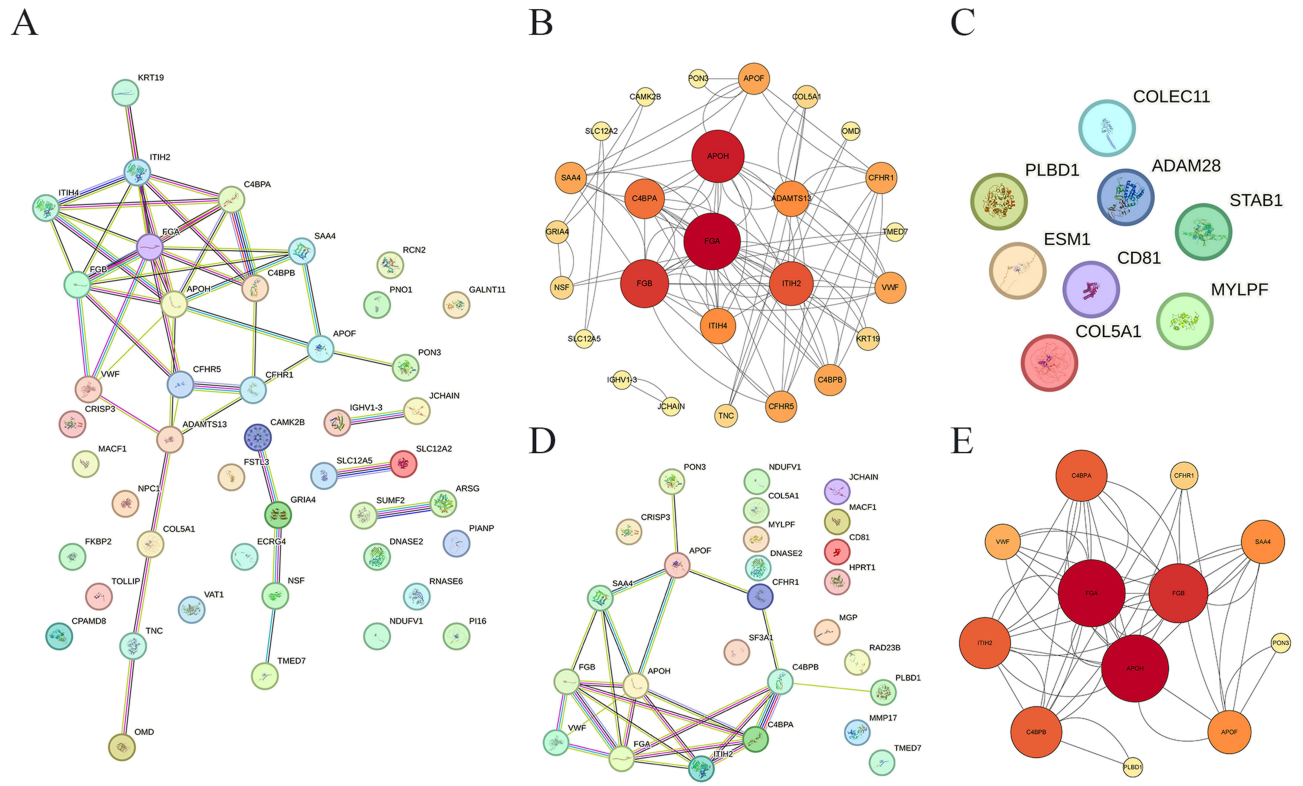

Figure 3 The interacted network of proteins analyzed by STRING. (**A**) STRING analysis of the relationship between the 53 specifically expressed proteins selected by the TBM group. (**B**) PPI analysis of the relationship between the 53 specifically expressed proteins selected by the TBM group. (**C**) STRING analysis of the relationship between the 9 specifically expressed proteins selected by the PM group. (**D**) STRING analysis of the relationship between the 29 specifically expressed proteins selected by the VM group. (**E**) PPI analysis of the relationship between the 29 specifically expressed proteins selected by the VM group.

ROC curve analysis revealed that when comparing the TBM group with the control group, FGA, FGB, C4BPA, and ADAMTS13 all achieved AUC values of 1.000. When compared with the non-TBM group, FGA and FGB also achieved a perfect AUC value of 1.000, while C4BPA and ADAMTS13 demonstrated highly favorable AUC values of 0.926 and 0.963, respectively. Collectively, these findings indicate that FGA, FGB, C4BPA, and ADAMTS13 exhibit outstanding discriminatory capability in differentiating TBM from non-TBM cases (Figure 5A–D). Similarly, in the analysis of the PM group, COLEC11 and ESM1 both achieved perfect AUC values of 1.000 when compared with the control group. Against the non-PM group, COLEC11 maintained a perfect AUC of 1.000, while ESM1 showed a high diagnostic accuracy with an AUC of 0.926. These results collectively indicate outstanding discriminatory capability of both

Table 5 Comparative Analysis of Candidate Proteins in TBM, PM, VM and Control Groups

Protein	TBM	PM	VM	Control
FGA	137.88(128.62, 171.92) ^{bbcddd}	71.35(24.80, 100.18) ^{aad}	88.82(78.99–88.83) ^{add}	21.52(22.08, 16.37) ^{aaabcc}
FGB	398.51±76.51 ^{bbccddd}	160.37±115.78 ^{aadd}	146.38±25.35 ^{aadd}	33.24±0.69 ^{aaabbcc}
C4BPA	54.65(36.55, 65.35) ^{bbcdd}	20.45(3.56, 24.62) ^{aad}	16.84(16.62–29.89) ^{add}	3.22(2.62, 3.68) ^{aabcc}
ADAMTS13	3.75±0.49 ^{bbccdd}	1.53±1.20 ^{aa}	1.34±0.39 ^{aa}	1.01±0.18 ^{aa}
COLEC11	0.73±0.18 ^{bb}	1.73±0.40 ^{aaccd}	0.63±0.38 ^{bb}	0.90±0.14 ^{b}
ESM1	0.25±0.21 ^{b}	0.72±0.18 ^{acd}	0.31±0.13 ^{b}	0.35±0.11 ^{b}
TMED7	0.52±0.04 ^{ccd}	0.85±0.33 ^{c}	1.85±0.33 ^{aabd}	1.08±0.27 ^{ac}
MMP17	0.54(0.20, 0.56) ^{c}	0.47(0.20, 0.60) ^{c}	0.87(0.21, 0.89) ^{abd}	0.53(0.52–0.55) ^{c}
CD81	0.42±0.36 ^{c}	0.68±0.07 ^{cd}	1.23±0.21 ^{abd}	0.34±0.11 ^{bc}

Notes: Compared with the TBM group, $^{a}P<0.05$; $^{aa}P<0.01$; $^{aaa}P<0.001$; Compared with the PM group, $^{b}P<0.05$; $^{bb}P<0.01$; Compared with the VM group, $^{c}P<0.05$; $^{cc}P<0.01$; Compared with the Control group, $^{d}P<0.05$; $^{dd}P<0.01$; $^{ddd}P<0.001$.

https://doi.org/10.2147/IDR.S570645

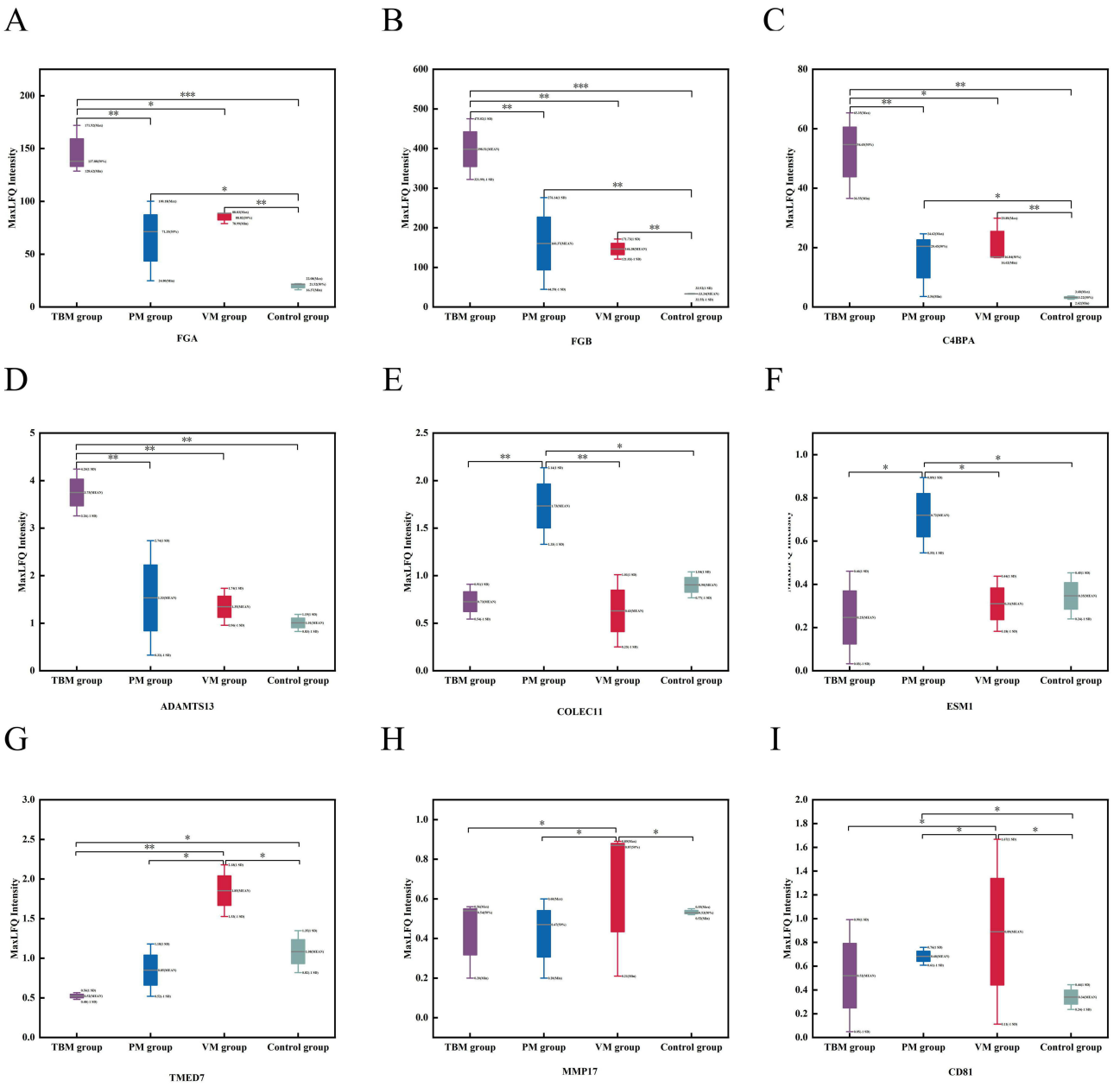

Figure 4 Expression boxplots of the 9 specifically expressed proteins in the four groups. (**A**) The boxplot of FGA. (**B**) The boxplot of FGB. (**C**) The boxplot of C4BPA. (**D**) The boxplot of ADAMTS13. (**E**) The boxplot of COLEC11. (**F**) The boxplot of ESM1. (**G**) The boxplot of TMED7. (**H**) The boxplot of MMP17. (**I**) The boxplot of CD81. SD: standard deviation. * *P*<0.05; ** *P*<0.01; *** *P*<0.001.

biomarkers in differentiating PM group from non-PM group (Figure 5E and F). In the VM group analysis, TMED7 demonstrated a perfect AUC of 1.000 compared to control group. While MMP17 and CD81 showed moderate diagnostic performance with AUC of 0.667 each. When comparing the VM group with the non-VM group, TMED7 once again achieved a perfect AUC of 1.000, confirming its exceptional discriminatory capability in distinguishing VM from non-VM group. Meanwhile, MMP17 and CD81 exhibited modest diagnostic utility with AUC values of 0.704 and 0.685 respectively, also showing a certain ability of differential diagnosis (Figure 5G–I).

Figure 6 shows the correlation heat map based on data normalization processing, including intra-group and inter-group comparisons. In intra-group correlation (Figure 6A), the protein-protein correlation heat map showed significant positive correlation among FGA, FGB, C4BPA and ADAMTS13 in the TBM group, implying their involvement in TBM biological processes. In the PM group, COLEC11 and ESM1 exhibited strong positive correlation, while TMED7,

https://doi.org/10.2147/IDR.S570645

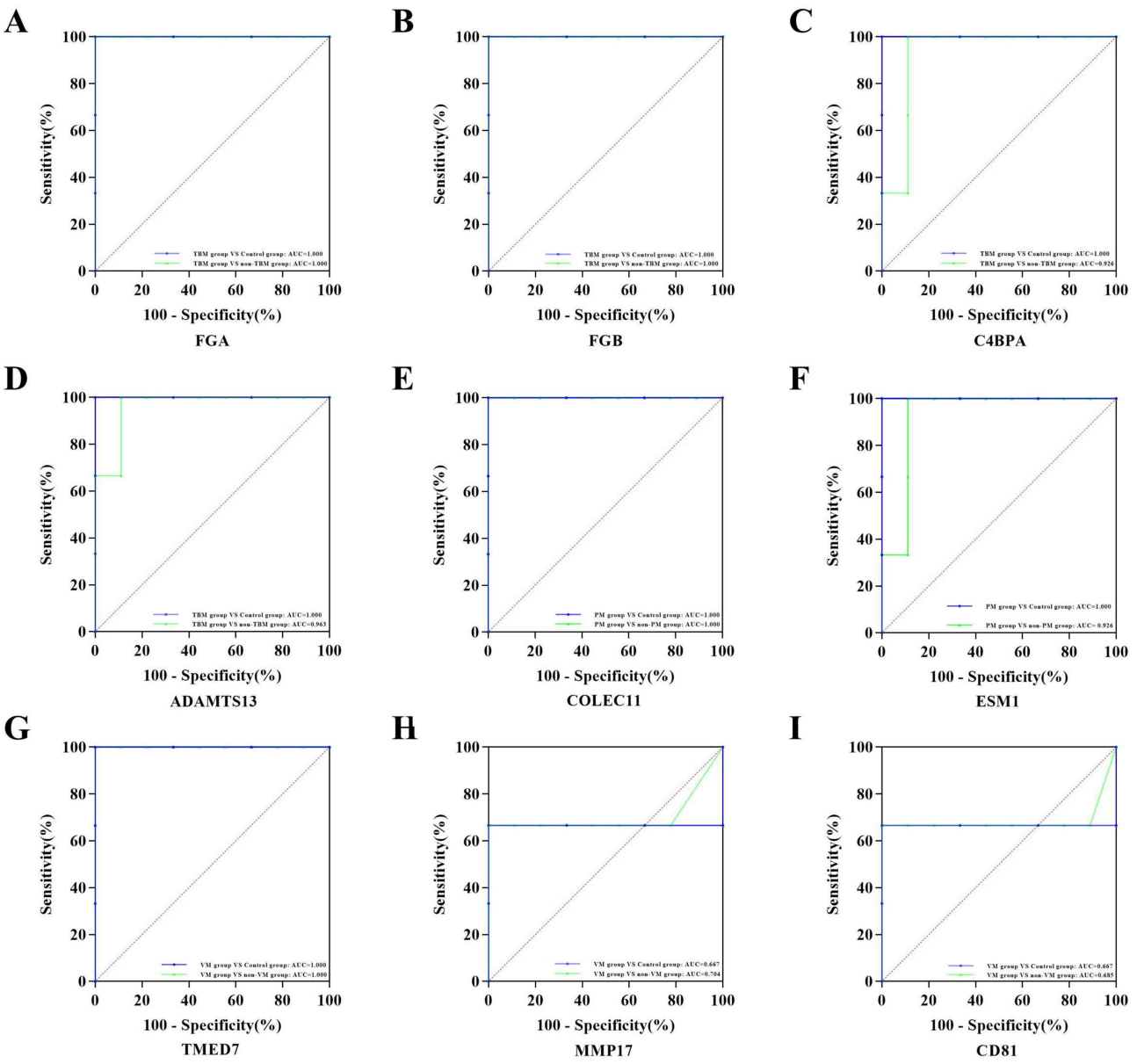

Figure 5 ROC curves of the 9 specifically expressed proteins. (**A**–**D**) ROC curves for FGA, FGB, C4BPA, and ADAMTS13 in differentiating the TBM group from the Control group and non-TBM group. (**E** and **F**) ROC curves for COLEC11 and ESM1 in differentiating the PM group from the Control group and non-PM group. (**G**–**I**) ROC curves for TMED7, MMP17, and CD81 in differentiating the VM group from the Control group and non-VM group.

MMP17, and CD81 in the VM group exhibited weak correlation. The inter-group correlation heat map further demonstrates the correlations of these proteins among different groups (Figure 6B). The heat map analysis revealed significant differences in the dimensions of specific proteins across various groups: FGA, FGB, C4BPA, and ADAMTS13 in the TBM group; COLEC11 and ESM1 in the PM group; and TMED7, MMP17, and CD81 in the VM group. Notably, each of these protein dimensions exhibited distinct variations when compared to those in the other groups. Critically, these distinct inter-group correlation patterns are highly consistent with the results of quantitative expression differences shown by the box plot.

Discussion

Our study revealed that the levels of white blood cells, red blood cells, IgG, NE%, and LY% in CSF were significantly elevated in the TBM, PM, and VM groups compared to the Control group. However, these indicators did not exhibit

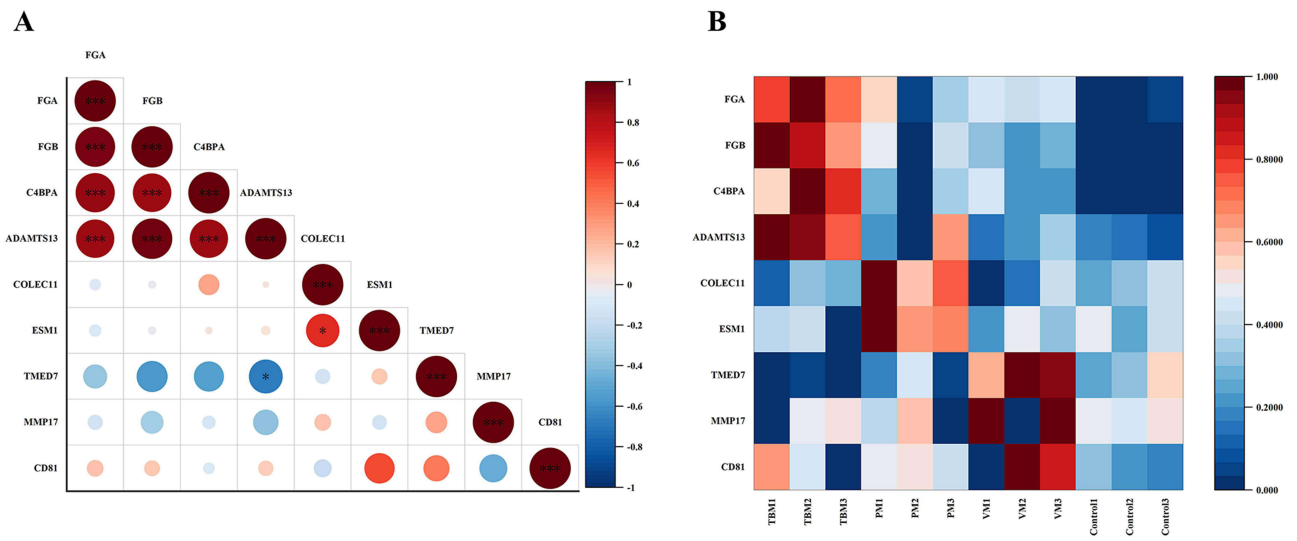

Figure 6 Heat map. (**A**) Heat map of correlations among the 9 specifically expressed proteins (* $P<0.05$; *** $P<0.001$). (**B**) Heat maps of 9 specifically expressed proteins in the TBM group, PM group, VM group and Control group.

statistically significant differences among the three types of meningitis. This finding suggests that conventional CSF laboratory tests, while useful for indicating the presence of meningitis, have limitations in differentiating among the different types of meningitis. In addition, our study found although ADA and TP levels exhibit variability across different types of meningitis, these measures alone are insufficient to fully distinguish between TBM, PM, and VM. Consequently, the search for more specific and sensitive diagnostic tools has become particularly imperative.

In recent years, proteomic techniques have gained increasingly application in meningitis research, particularly for early diagnosis and etiology identification. Numerous studies have employed proteomic techniques to analyze CSF proteins for specific biomarkers. For example, Liu et al conducted a proteomic analysis of the CSF in patients with varicella zoster virus (VZV) meningitis and those with herpes zoster,[22] revealing inflammatory immune response as a key pathophysiological mechanism of VZV infection in the CNS and suggesting CSF IL-18 levels as a potential prognostic indicator of VZV meningitis. Mu et al used iTRAQ labeling combined with LC-MS/MS technology to show significantly upregulated CSF levels of FGA, FGB, and ITIH4 proteins in TBM patients compared to healthy controls.[23] However, these studies focus on single diseases or limited subtypes, lacking comprehensive comparisons across multiple meningitis types. This limitation restricts the broad applicability of their findings to different meningitis subtypes. Compared with previous studies that mainly focused on a single CNS infection disease, this study employed 4D-DIA technology to perform proteomic analysis of CSF from patients with TBM, PM, VM, and non-CNS infections. Our study identified significantly different proteins among the three types of meningitis, and the differential expression patterns observed in the CSF of patients with CNS infections were closely correlated with their functions. These findings enhance our understanding of the biological pathways underlying central nervous system infections, identify potential biomarkers for each type of meningitis, and provide valuable insights for clinical diagnosis and treatment.

The following sections discuss the proteins of interest identified in our exploratory analysis. It is crucial to emphasize that their associations with disease mechanisms are proposed based on existing literature and bioinformatics, and their roles as specific diagnostic biomarkers remain to be prospectively validated.

Regarding the proteomic signature of TBM, an independent investigation employing iTRAQ-LC-MS/MS proteomic analysis of CSF revealed significant upregulation of FGA, FGB, C4BPA, and ITIH4 in TBM patients compared to healthy controls. Bioinformatics interrogation further demonstrated enrichment of these differentially expressed proteins in immune-inflammatory pathways, notably the complement and coagulation cascades and cell adhesion molecules.[24] It is worth noting that our study is highly consistent with the above findings: FGA, FGB, C4BPA and ADAMTS13 are not only the key hub proteins of the PPI network in the CSF of the TBM group, but their expression levels are also significantly higher than those of other groups ($P < 0.05$). Furthermore, ROC curve analysis substantiated the diagnostic

https://doi.org/10.2147/IDR.S570645

utility of these biomarkers. Both FGA and FGB exhibited perfect discriminatory power for TBM identification (AUC = 1.000), while C4BPA (AUC = 0.926) and ADAMTS13 (AUC = 0.963) also displayed outstanding diagnostic efficacy. Collectively, these proteins illuminate distinct pathophysiological mechanisms underlying TBM and present promising novel diagnostic targets. FGA and FGB encode the α and β chains of fibrinogen, respectively, which is a crucial precursor protein in the coagulation process.[25] The elevated levels of FGA and FGB of TBM patients may be related to the local inflammatory response and fibrin deposition induced by tuberculosis infection. KEGG pathway analysis revealed that FGA and FGB are involved in the complement and coagulation cascade, as well as the coronavirus disease-COVID-19 pathway among TBM patients. The activation of the complement and coagulation cascades plays a crucial role in the body's defense against Mycobacterium tuberculosis infection. Nonetheless, excessive activation of the complement system may result in tissue damage and prolonged inflammatory responses. Concurrently, aberrant activation of the coagulation cascade may lead to thrombosis in the brain, thereby further compromising CNS function. In addition, the involvement of FGA and FGB in the COVID-19 pathway suggests a potential overlap in inflammatory response and immune mechanism between TBM and COVID-19. For instance, during COVID-19, fibrinogen is significantly linked to the hyperactivation of immune response alongside aberrant coagulation,[26] Similar phenomena have also been observed in TBM. This finding suggests the potential interaction between infectious diseases and provides new clues for further exploration into their common underlying mechanisms. C4BPA acts as a regulatory factor in the classical complement pathway, inhibiting excessive activation of the complement cascade by binding to C4b.[27,28] In patients with TBM, elevated levels of C4BPA may indicate a component of the body's immunomodulatory response to Mycobacterium tuberculosis infection. Moderate activation of the complement system is crucial for pathogen clearance, but excessive activation may lead to tissue damage.[29] Consequently, elevated levels of C4BPA reflect a complex mechanism that balances the immune response with tissue protection. ADAMTS13 functions as a metalloproteinase that cleaves Von Willebrand factor (VWF) polymers, thereby preventing the formation of abnormal thrombi.[30,31] In patients with TBM, elevated ADAMTS13 levels may be associated with blood-brain barrier damage and vascular endothelial dysfunction. Given that TBM is usually associated with vascular lesions, the high expression of ADAMTS13 may be a regulatory response by the body to an abnormal coagulation mechanism. This response potentially prevents the formation of pathological thrombosis and reduces brain injury resulting from vascular endothelial dysfunction.[32] This mechanism further supports the hypothesis that coagulation and fibrinolysis systems may be activated in TBM. In conclusion, the elevated levels of FGA and FGB indicate activation of the coagulation system in TBM, which is intricately linked to the inflammatory response induced by Mycobacterium tuberculosis infection and subsequent blood-brain barrier disruption. Additionally, the increased concentration of C4BPA may reflect the regulatory function of the complement system in TBM, further supporting the significant role of inflammation and immune response in the disease's pathogenesis. Furthermore, the heightened levels of ADAMTS13 suggest that, in the context of TBM, the body may respond to the risk of clotting caused by blood-brain barrier damage and inflammation by regulating thrombosis. The high expression of these hub proteins in TBM patients not only reflects the pathophysiological characteristics of TBM, but also suggests that they can be used as potential biomarkers for the early diagnosis of TBM.

In PM research, Anahita Bakochi et al established a CSF proteomic atlas, revealing distinct alterations in the CSF proteome across meningitis etiologies. Compared to VM, proteins differentially expressed in PM were predominantly enriched in biological processes including regulation of apoptotic signaling pathways, glial cell development, and defense response to bacteria. Furthermore, among 18 PM-associated proteins selected via LASSO regression, nine exhibited specific elevation in PM patients. These included proteins implicated in inflammatory responses (A2GL, HPT A1T1), fibrin clot formation (HEP2, PROS), LPS binding (CD14), and regulation of the complement cascade (CFAH). A diagnostic panel incorporating these markers achieved exceptional discriminative power (AUC = 0.96) for early PM detection.[33] Notably, our study extends these findings by identifying significantly elevated expression levels of COLEC11 and ESM1 in PM patients compared to other groups ($P < 0.05$). This suggests their potential involvement in PM-specific immune-pathological mechanisms. ROC analysis further highlighted their diagnostic potential: COLEC11 demonstrated exceptional discriminatory capacity for PM (AUC = 1.000), while ESM1 also showed high diagnostic efficacy (AUC = 0.926). Collectively, COLEC11 and ESM1 represent promising novel biomarkers for the rapid differential diagnosis of PM. COLEC11, a pattern recognition molecule belonging to the lectin family, plays

a distinctive role in host defense, embryonic development, and acute inflammation.[34] Pathogen recognition constitutes a critical step in host defense against pathogens.[35] COLEC11 can recognize and bind to the pathogens and host cell surface carbohydrates (eg, monosaccharides, mannose-containing glycans, lipopolysaccharides, DNA, microorganisms), thus activating the lectin pathway of complement cascade reaction.[36] The activation of this pathway not only augments the inflammatory response but also enhances T cell activation and improves the host's pathogen clearance capabilities.[37] Our findings corroborate these results, with KEGG pathway analysis indicates that COLEC11 is implicated in the phagosome signaling pathway in the context of PM. Phagosomes are vesicles internalized by cells via phagocytosis, which could fuse with lysosomes during maturation to form phagolysosomes to kill and digest pathogenic microorganisms.[38] Consequently, elevated levels of COLEC11 in PM patients reflect the rapid bacterial recognition and subsequent immune response. ESM1 is a proteoglycan-structured molecule whose secretion is regulated by pro-inflammatory molecules, including tumor necrosis factor (TNF)-α, interleukin (IL)-1, E-selectin, and other cellular mediators such as bacterial lipopolysaccharide, angiogenesis factors, vascular endothelial growth factor (VEGF), or fibroblast growth factor (FGF)-2.[39] ESM1 primarily facilitates the transport of inflammatory molecules at the endothelial cell levels, regulates cell adhesion, migration, proliferation and neo-vascularization, thereby playing a regulatory role in endothelial activation and dysfunction.[40] Dysregulation of ESM1 expression has been substantiated to be associated with various pathological mechanisms including angiogenesis, vascular remodeling, inflammation, and atherosclerosis.[41] In the context of PM, elevated levels of ESM1 indicate endothelial cell dysfunction and increased inflammatory mediators.

For VM, Wang et al employed DIA mass spectrometry to analyze CSF from enterovirus-positive patients, identifying 816 proteins (66 upregulated and 108 downregulated). Differentially expressed proteins were primarily associated with the complement and coagulation cascades, cell signal transduction, and response to infection.[42] Our study also observed a similar mechanism. KEGG pathway analysis similarly revealed significant enrichment of differentially expressed proteins in the complement and coagulation cascade pathway within the VM group. Furthermore, we identified significantly elevated expression levels of TMED7, MMP17, and CD81 in the CSF of VM patients compared to other groups ($P< 0.05$). This suggests their potential involvement in the pathophysiological processes of VM. ROC analysis further evaluated their diagnostic potential. TMED7 demonstrated exceptional discriminatory capacity for VM (AUC = 1.000), while MMP17 (AUC = 0.704) and CD81 (AUC = 0.685) exhibited modest diagnostic potential. These results position TMED7 as a highly efficient diagnostic biomarker for VM, with MMP17 and CD81 potentially providing supplementary diagnostic information. MMP17 is a member of the membrane-type matrix metalloproteinases (MT-MMPs) family. Proteases of this family are integral to the degradation of the extracellular matrix, intercellular adhesion, and cytokine signaling.[43] Recent investigations have demonstrated a significant correlation between MMP17 expression and extracellular matrix degradation, as well as skeletal system development.[44] Furthermore, MMP17 has been implicated in angiogenesis and inflammation, playing a role in the pathogenesis of various diseases including osteoarthritis, atherosclerosis, thoracic aortic aneurysm, and dissection.[45] The upregulation of MMP17 in patients with VM may be related to the inflammatory response and tissue remodeling induced by viral infection.[46] MMP17 facilitates the degradation of the extracellular matrix and increases the permeability of the blood-brain barrier, thereby promoting the infiltration of inflammatory cells and enhancing the antiviral immune response. TMED7 is a crucial member of the p24 protein family, known for its role as a transport factor for various cargoes. Abnormal expression of TMED proteins has been associated with immune disorders, cancer, liver diseases, and pancreatic disorders.[47,48] In our study, we observed higher levels of TMED7 in the CSF of patients with VM compared to other groups. This elevation is hypothesized to be due to the increased requirement for protein transport and regulation during virus replication and assembly within host cells.[49,50] As a membrane protein involved in protein transport and secretion, TMED7 may be upregulated to facilitate the formation and release of viral particles during viral replication and packaging. Notably, our study observed elevated levels of CD81 in patients with VM compared to other groups. As a four-transmembrane protein, CD81 is a co-receptor for several viruses, including hepatitis C virus (HCV), human immunodeficiency virus type 1 (HIV-1), herpes simplex virus type 1 (HSV-1), influenza A virus (IAV) and a few others.[51] CD81 is instrumental in facilitating the entry of these viruses into host cells. In addition, CD81 can also affect the immune response post-infection by regulating the activation of immune cells and inflammatory response. Studies have shown that on the surface of a B-cell, CD81 participates in forming CD19-signaling complex, which works in conjunction with the B-cell antigen receptor (BCR) to lower the activation threshold of BCR, thereby promoting antibody production in response to antigenic stimulation.[52,53] Elevated levels

of CD81 in VM may reflect the stress response of the CNS to viral infection and its regulatory function in the inflammatory process.

The complement system is a key component of the innate immune response and is activated through three main pathways: the classical, alternative, and lectin pathways. These pathways promote pathogen clearance, immune regulation, and tissue repair.[54] In our study, IGLC7, C4BPA, C4BPB and IGHV1-8 were identified as specific expressed proteins in the TBM and VM groups, mediating the classical pathway of complement activation, whereas in the PM group, these specific proteins did not show significant activation of the classical pathway. This finding provides a new perspective for further understanding the immunopathological mechanisms of each subtype of meningitis. With respect to TBM, Mycobacterium tuberculosis, as an intracellular parasite, has an antigenic component that participates in the immune response by activating the classical complement pathway.[55] The formation of the antigen-antibody complex can effectively activate the C1 complex, which in turn triggers the downstream complement cascade, producing active fragments such as C3b and membrane attack complexes (MAC) that help clear infected cells and limit the spread of pathogens.[56] Similarly, in viral meningitis (VM), new epitopes may appear on the surface of host cells after viral infection, inducing the production of antiviral antibodies and thus initiating the classical complement pathway.[57] The effects of complement activation help identify and clear virus-infected cells, limiting the spread of the virus. PM is usually caused by infection with bacteria whose cell wall components (such as lipopolysaccharides, peptidoglycans, etc.) are highly immunogenic and can directly activate the bypass and lectin pathways of the complement system, triggering a rapid and intense inflammatory response.[58] In this case, PM-specifically expressed proteins may be more involved in immunomodulatory processes associated with the bypass pathway or the lectin pathway, but not significantly involved in the activation of the classical pathway. In summary, our findings highlight the differences in complement activation mechanisms among different subtypes of meningitis, which contribute to a deeper understanding of the unique pathogenesis of each subtype of meningitis.

Limitations and Future Perspectives

Despite providing valuable insights into the proteomic signatures and potential biomarkers of meningitis subtypes, this study has several limitations. First, the cases included were sourced from a single center with a relatively small sample size, which may impact the detection efficiency of inter-group comparisons and increase the risk of overfitting. Additionally, although the pooled-sample design is necessary for deep proteomic coverage, it impairs the assessment of individual variability.

Future research should expand the sample size and incorporate data from multiple centers to enhance the reliability and clinical applicability of the findings. Furthermore, it is essential to conduct in vitro functional experiments and in vivo animal model studies to elucidate the biological functions and clinical translational potential of these candidate markers. By implementing these enhancements, future research is anticipated to offer a more robust theoretical foundation and practical guidance for the precise diagnosis and treatment of CNS infections.

Conclusion

This study delineated the CSF protein profiles in patients with TBM, PM, VM, and non-CNS infections. We identified several potential biomarkers, including FGA, FGB, C4BPA, ADAMTS13, COLEC11, ESM1, TMED7, MMP17, and CD81. Additionally, we proposed hypothetical molecular mechanisms that may offer valuable diagnostic and therapeutic insights for CNS infections. Nonetheless, given that this is a preliminary exploratory study, further validation through multicenter, large-sample cohort studies and functional experiments is necessary to substantiate the clinical relevance and utility of these biomarkers prior to any potential application in clinical practice.

Data Sharing Statement

The datasets generated during and/or analyzed during the current study are available from the corresponding author on reasonable request.

Ethics Statement

This study complies with the Declaration of Helsinki and was approved by the Medical Ethics Committee of Gansu Provincial Hospital (Approval No. 2024-308).

Author Contributions

All authors made a significant contribution to the work reported, whether that is in the conception, study design, execution, acquisition of data, analysis and interpretation, or in all these areas; took part in drafting, revising or critically reviewing the article; gave final approval of the version to be published; have agreed on the journal to which the article has been submitted; and agree to be accountable for all aspects of the work.

Funding

Research Foundation for Talented Scholars of Gansu Provincial Hospital (2024KYQDJ-B-11).

Disclosure

The authors declare that the research was conducted in the absence of any commercial or financial relationships that could be construed as a potential conflict of interest.

References

1. Venkatesan P. Defeating meningitis by 2030: the WHO roadmap. *Lancet Infect Dis*. 2021;21(12):1635. PMID 34838228. doi:10.1016/s1473-3099(21)00712-x
2. Li S, Nguyen IP, Urbanczyk K. Common infectious diseases of the central nervous system-clinical features and imaging characteristics. *Quant Imaging Med Surg*. 2020;10(12):2227–2259. PMID 33269224. doi:10.21037/qims-20-886
3. Wang Q, Lin Q, Wang H, et al. Diagnostic value of cerebrospinal fluid neutrophil gelatinase-associated lipocalin for differentiation of bacterial meningitis from tuberculous meningitis or cryptococcal meningitis: a prospective cohort study. *J Transl Med*. 2023;21(1):603. PMID 37679727. doi:10.1186/s12967-023-04485-w
4. Na S, Kim T, Song IU, et al. The association between serum sodium level and tuberculous meningitis compared with viral and bacterial meningitis. *Sci Rep*. 2021;11(1):10906. PMID 34035388. doi:10.1038/s41598-021-90358-5
5. Xing XW, Zhang JT, Ma YB, et al. Metagenomic next-generation sequencing for diagnosis of infectious encephalitis and meningitis: a large, prospective case series of 213 patients. *Front Cell Infect Microbiol*. 2020;10:88. PMID 32211343. doi:10.3389/fcimb.2020.00088
6. Kozioł A, Pupek M, Lewandowski Ł. Application of metabolomics in diagnostics and differentiation of meningitis: a narrative review with a critical approach to the literature. *Biomed Pharmacother*. 2023;168:115685. PMID 37837878. doi:10.1016/j.biopha.2023.115685
7. van Zeggeren IE, Edridge AWD, van de Beek D, et al. Diagnostic accuracy of VIDISCA-NGS in patients with suspected central nervous system infections. *Clin Microbiol Infect*. 2021;27(4):631.e7–631.e12. PMID 32590059. doi:10.1016/j.cmi.2020.06.012
8. Zhang L, Zhang Y, Wang X, Zhao Y. Correlation of levels of lactic acid and glucose in cerebrospinal fluid of cerebral hemorrhage patients with the occurrence of postoperative intracranial infection and clinical prognosis. *J Med Biochem*. 2024;43(1):36–42. PMID 38496025. doi:10.5937/jomb0-44058
9. Yekani M, Memar MY. Immunologic biomarkers for bacterial meningitis. *Clin Chim Acta*. 2023;548:117470. PMID 37419301. doi:10.1016/j.cca.2023.117470
10. Yim YY, Nestler EJ. Cell-type-specific neuroproteomics of synapses. *Biomolecules*. 2023;13(6). PMID 37371578. doi:10.3390/biom13060998
11. Li KW, Ganz AB, Smit AB. Proteomics of neurodegenerative diseases: analysis of human post-mortem brain. *J Neurochem*. 2019;151(4):435–445. PMID 30289976. doi:10.1111/jnc.14603
12. Lee H, Kim SI. Review of liquid chromatography-mass spectrometry-based proteomic analyses of body fluids to diagnose infectious diseases. *Int J Mol Sci*. 2022;23(4). PMID 35216306. doi:10.3390/ijms23042187
13. Ahmed S, van Zalm P, Rudmann EA, et al. Using CSF proteomics to investigate herpesvirus infections of the central nervous system. *Viruses*. 2022;14(12):2757. PMID 36560759. doi:10.3390/v14122757
14. Gómez-Baena G, Bennett RJ, Martínez-Rodríguez C, et al. Quantitative proteomics of cerebrospinal fluid in paediatric pneumococcal meningitis. *Sci Rep*. 2017;7(1):7042. PMID 28765563. doi:10.1038/s41598-017-07127-6
15. Kumar GS, Venugopal AK, Mahadevan A, et al. Quantitative proteomics for identifying biomarkers for tuberculous meningitis. *Clin Proteomics*. 2012;9(1):12. PMID 23198679. doi:10.1186/1559-0275-9-12
16. Xie H, Zhang Y, Zhu Z, Wei J, Ainiwaer G, Ge W. Plasma proteomic analysis based on 4D-DIA evaluates the clinical response to imrecoxib in the early treatment of osteoarthritis. *Rheumatol Ther*. 2024;11(2):269–283. PMID 38236456. doi:10.1007/s40744-023-00636-z
17. Nolka-Szaszner M, Strugała A, Marczak Ł. Data-driven mass spectrometry methods (DDA) and data-independent methods (DIA) used in the analysis of biological material. *Postepy Biochem*. 2024;70(2):212–222. PMID 39083467. doi:10.18388/pb.2021_535
18. Cao Q, Zhu H, Xu W, et al. Predicting the efficacy of glucocorticoids in pediatric primary immune thrombocytopenia using plasma proteomics. *Front Immunol*. 2023;14:1301227. PMID 38162645. doi:10.3389/fimmu.2023.1301227
19. Walzer M, García-Seisdedos D, Prakash A, et al. Implementing the reuse of public DIA proteomics datasets: from the PRIDE database to expression atlas. *Sci Data*. 2022;9(1):335. PMID 35701420. doi:10.1038/s41597-022-01380-9

20. Aebersold R, Mann M. Mass-spectrometric exploration of proteome structure and function. *Nature*. 2016;537(7620):347–355. PMID 27629641. doi:10.1038/nature19949
21. Zhou R, Tu Z, Chen D, et al. Quantitative proteome and lysine succinylome characterization of zinc chloride smoke-induced lung injury in mice. *Heliyon*. 2024;10(6):e27450. PMID 38524532. doi:10.1016/j.heliyon.2024.e27450
22. Liu H, Wang J, Zhang Y, et al. Cerebrospinal fluid proteomics in meningitis patients with reactivated varicella zoster virus. *Immun Inflamm Dis*. 2023;11(10):e1038. PMID 37904697. doi:10.1002/iid3.1038
23. Mu J, Yang Y, Chen J, et al. Elevated host lipid metabolism revealed by iTRAQ-based quantitative proteomic analysis of cerebrospinal fluid of tuberculous meningitis patients. *Biochem Biophys Res Commun*. 2015;466(4):689–695. PMID 26348777. doi:10.1016/j.bbrc.2015.08.036
24. Yang Y, Mu J, Chen G, et al. iTRAQ-based quantitative proteomic analysis of cerebrospinal fluid reveals NELL2 as a potential diagnostic biomarker of tuberculous meningitis. *Int J Mol Med*. 2015;35(5):1323–1332. PMID 25760060. doi:10.3892/ijmm.2015.2131
25. Maners J, Gill D, Pankratz N, et al. A Mendelian randomization of γ' and total fibrinogen levels in relation to venous thromboembolism and ischemic stroke. *Blood*. 2020;136(26):3062–3069. PMID 33367543. doi:10.1182/blood.2019004781
26. Henderson MW, Lima F, Moraes CRP, et al. Contact and intrinsic coagulation pathways are activated and associated with adverse clinical outcomes in COVID-19. *Blood Adv*. 2022;6(11):3367–3377. PMID 35235941. doi:10.1182/bloodadvances.2021006620
27. Xie HG, Jiang LP, Tai T, Ji JZ, Mi QY. The complement system and C4b-binding protein: a focus on the promise of C4BPα as a biomarker to predict clopidogrel resistance. *Mol Diagn Ther*. 2024;28(2):189–199. PMID 38261250. doi:10.1007/s40291-023-00691-w
28. Ermert D, Blom AM. C4b-binding protein: the good, the bad and the deadly. Novel functions of an old friend. *Immunol Lett*. 2016;169:82–92. PMID 26658464. doi:10.1016/j.imlet.2015.11.014
29. Brennan FH, Anderson AJ, Taylor SM, Woodruff TM, Ruitenberg MJ. Complement activation in the injured central nervous system: another dual-edged sword? *J Neuroinflammation*. 2012;9:137. PMID 22721265. doi:10.1186/1742-2094-9-137
30. Papakonstantinou A, Kalmoukos P, Mpalaska A, Koravou EE, Gavriilaki E. ADAMTS13 in the new era of TTP. *Int J Mol Sci*. 2024;25(15):8137. PMID 39125707. doi:10.3390/ijms25158137
31. Otmani HE, Vanhoorelbeke K, Tersteeg C. Improving our understanding on the clinical role of plasmin-mediated von Willebrand factor degradation. *Curr Opin Hematol*. 2024;31(5):245–250. PMID 38723202. doi:10.1097/moh.0000000000000825
32. Rurali E, Noris M, Chianca A, et al. ADAMTS13 predicts renal and cardiovascular events in type 2 diabetic patients and response to therapy. *Diabetes*. 2013;62(10):3599–3609. PMID 23733198. doi:10.2337/db13-0530
33. Bakochi A, Mohanty T, Pyl PT, et al. Cerebrospinal fluid proteome maps detect pathogen-specific host response patterns in meningitis. *Elife*. 2021;10. PMID 33821792. doi:10.7554/eLife.64159
34. Gao B, Wang Y, Zhang X, et al. Identification and validation of inflammatory subtypes in intrahepatic cholangiocellular carcinoma. *J Transl Med*. 2024;22(1):730. PMID 39103879. doi:10.1186/s12967-024-05529-5
35. Sandri TL, Andrade FA, Lidani KCF, et al. Human collectin-11 (COLEC11) and its synergic genetic interaction with MASP2 are associated with the pathophysiology of chagas disease. *PLoS Negl Trop Dis*. 2019;13(4):e0007324. PMID 30995222. doi:10.1371/journal.pntd.0007324
36. Wu W, Liu C, Farrar CA, et al. Collectin-11 promotes the development of renal tubulointerstitial fibrosis. *J Am Soc Nephrol*. 2018;29(1):168–181. PMID 29142050. doi:10.1681/asn.2017050544
37. Fanelli G, Romano M, Lombardi G, Sacks SH. Soluble collectin 11 (CL-11) acts as an immunosuppressive molecule potentially used by stem cell-derived retinal epithelial cells to modulate T cell response. *Cells*. 2023;12(13):1805. PMID 37443840. doi:10.3390/cells12131805
38. Yang D, Fu X, He S, Ning X, Ling M. Analysis of differentially expressed proteins in mycobacterium avium-infected macrophages comparing with mycobacterium tuberculosis-infected macrophages. *Biomed Res Int*. 2017;2017:5103803. PMID 28573139. doi:10.1155/2017/5103803
39. Kechagia M, Papassotiriou I, Gourgoulianis KI. Endocan and the respiratory system: a review. *Int J Chron Obstruct Pulmon Dis*. 2016;11:3179–3187. PMID 28003744. doi:10.2147/copd.S118692
40. Constantin L, Ungurianu A, Streinu-Cercel A, et al. Investigation of serum endocan levels in SARS-CoV-2 patients. *Int J Mol Sci*. 2024;25(5):3042. PMID 38474287. doi:10.3390/ijms25053042
41. Salzinger B, Lundwall K, Evans M, et al. Associations between inflammatory and angiogenic proteomic biomarkers, and cardiovascular events and mortality in relation to kidney function. *Clin Kidney J*. 2024;17(3):sfae050. PMID 38524235. doi:10.1093/ckj/sfae050
42. Wang YL, Guo XT, Zhu MY, et al. Metagenomic next-generation sequencing and proteomics analysis in pediatric viral encephalitis and meningitis. *Front Cell Infect Microbiol*. 2023;13:1104858. PMID 37153144. doi:10.3389/fcimb.2023.1104858
43. Li W, Liu Y, Xu X, et al. The relationship between MMP17 variants and ischemic stroke risk in the population from Shaanxi Province in China. *Pharmgenomics Pers Med*. 2023;16:59–66. PMID 36733691. doi:10.2147/pgpm.S396076
44. Xiao C, Wang Y, Cheng Q, Fan Y. Increased expression of MMP17 predicts poor clinical outcomes in epithelial ovarian cancer patients. *Medicine*. 2022;101(34):e30279. PMID 36042626. doi:10.1097/md.0000000000030279
45. Yip C, Foidart P, Noël A, Sounni NE. MT4-MMP: the GPI-anchored membrane-type matrix metalloprotease with multiple functions in diseases. *Int J Mol Sci*. 2019;20(2):354. PMID 30654475. doi:10.3390/ijms20020354
46. Blanco MJ, Rodríguez-Martín I, Learte AIR, et al. Developmental expression of membrane type 4-matrix metalloproteinase (Mt4-mmp/Mmp17) in the mouse embryo. *PLoS One*. 2017;12(9):e0184767. PMID 28926609. doi:10.1371/journal.pone.0184767
47. Zhou L, Li H, Yao H, Dai X, Gao P, Cheng H. TMED family genes and their roles in human diseases. *Int J Med Sci*. 2023;20(13):1732–1743. PMID 37928880. doi:10.7150/ijms.87272
48. Mota D, Cardoso IA, Mori RM, et al. Structural and thermodynamic analyses of human TMED1 (p24γ1) Golgi dynamics. *Biochimie*. 2022;192:72–82. PMID 34634369. doi:10.1016/j.biochi.2021.10.002
49. Liu YY, Bai JS, Liu CC, et al. The small GTPase Rab14 regulates the trafficking of ceramide from endoplasmic reticulum to golgi apparatus and facilitates classical swine fever virus assembly. *J Virol*. 2023;97(5):e0036423. PMID 37255314. doi:10.1128/jvi.00364-23
50. Boson B, Legros V, Zhou B, et al. The SARS-CoV-2 envelope and membrane proteins modulate maturation and retention of the spike protein, allowing assembly of virus-like particles. *J Biol Chem*. 2021;296:100111. PMID 33229438. doi:10.1074/jbc.RA120.016175
51. Bailly C, Thuru X. Targeting of tetraspanin CD81 with monoclonal antibodies and small molecules to combat cancers and viral diseases. *Cancers*. 2023;15(7):2186. PMID 37046846. doi:10.3390/cancers15072186
52. Yeung L, Hickey MJ, Wright MD. The many and varied roles of tetraspanins in immune cell recruitment and migration. *Front Immunol*. 2018;9:1644. PMID 30072994. doi:10.3389/fimmu.2018.01644

53. Zona L, Tawar RG, Zeisel MB, et al. CD81-receptor associations--impact for hepatitis C virus entry and antiviral therapies. *Viruses*. 2014;6 (2):875–892. PMID 24553110. doi:10.3390/v6020875
54. Rahmati Nezhad P, Riihilä P, Knuutila JS, et al. Complement factor D is a novel biomarker and putative therapeutic target in cutaneous squamous cell carcinoma. *Cancers*. 2022;14(2). PMID 35053469. doi:10.3390/cancers14020305
55. Wu S, Liu X, Chen L, et al. Polymorphisms of TLR2, TLR4 and TOLLIP and tuberculosis in two independent studies. *Biosci Rep*. 2020;40(8). PMID 32648572. doi:10.1042/bsr20193141
56. Noone DP, Dijkstra DJ, van der Klugt TT, et al. PTX3 structure determination using a hybrid cryoelectron microscopy and AlphaFold approach offers insights into ligand binding and complement activation. *Proc Natl Acad Sci U S A*. 2022;119(33):e2208144119. PMID 35939690. doi:10.1073/pnas.2208144119
57. Shi J, Chu C, Yu M, et al. Clinical warning of hemophagocytic syndrome caused by Epstein-Barr virus. *Ital J Pediatr*. 2021;47(1):3. PMID 33413556. doi:10.1186/s13052-020-00949-7
58. Younger JG, Shankar-Sinha S, Mickiewicz M, et al. Murine complement interactions with Pseudomonas aeruginosa and their consequences during pneumonia. *Am J Respir Cell Mol Biol*. 2003;29(4):432–438. PMID 14500254. doi:10.1165/rcmb.2002-0145OC